THE DESIGN AND CONSTRUCTION OF A LABORATORY FACILITY FOR THE MEASUREMENT OF REACTOR MODERATOR PARAMETERS

by

Lee Saunders Anthony

Thesis submitted to the Graduate Faculty of the

Virginia Polytechnic Institute

in candidacy for the degree of

MASTER OF SCIENCE

in

Nuclear Engineering Physics

APPROVED:

Director of Graduate Studies

Dean of Applied Science, and Business Administration

APPROVED:

Head of Department

Dean of Engineering and Architecture

Supervisor or Major Professor

May 14, 1958

Blacksburg, Virginia

II TABLE OF CONTENTS

II TABLE OF CONTENTS (con't)

III INTRODUCTION

The study and applications of Nuclear Engineering have become increasingly important in world affairs, especially from considerations of power and economics. Foreseeing the needs of men trained in engineering applications of nuclear principles, many schools, with the aid of the Atomic Energy Commission, have instituted programs for the training of such specialists.

Virginia Polytechnic Institute was among the early schools to initiate such a program, offering a Master of Science program in Nuclear Engineering Physics in September, 1956.

The first major departmental acquisition for this purpose was an exponential graphite-moderated natural-uranium reactor.

Suitable equipment was next obtained to provide facilities for modern nuclear and reactor physics laboratories. This equipment includes a nuclear reactor simulator, and counting equipment.

It was next decided to add a "Sigma Pile" to the reactor laboratory. Graphite was chosen as the moderator for ease of handling, low cost, ease of precise machining, and because it is possible to obtain graphite of sufficient purity in quantity.

The sigma pile is eight feet high and sixty-six inches square. AGOT reactor grade graphite was used for its construction.

The Pile was constructed during the fall of 1957 and was ready for use by the reactor laboratory students in January, 1958. The students used the pile for determination of diffusion length and Fermi age.

IV REVIEW OF LITERATURE

Sigma piles have historically been used for the determination of cross sections, from whence comes the name, "sigma."

Since it is economical to accomplish as much as possible on new reactors by calculations rather than by experiment, and in order to predict behavior of materials, it is of major concern to all in the field to know their properties or parameters as accurately as possible.

In the sigma pile, the observed neutron distribution is used to obtain the thermal diffusion length (41), from which can be calculated either the absorption cross section or transport cross section from (42),

$$L = \frac{1}{(3N^2\sigma_a\sigma_{tr})^{\frac{1}{2}}}$$

where L = diffusion length

N = nuclei per cm^3

σ_a = microscopic absorption cross section

σ_{tr} = microscopic transport cross section

which is one definition of diffusion length.

One major drawback is the relatively low flux of the sigma pile compared to the flux in a thermal column or reactor.

As would be expected, much work has been done using sigma pile techniques, especially at Hanford, Brookhaven, and Oak Ridge. Among those who have contributed much to the field are D. J. Hughes (40), J. Chernick and I. Kaplan (11), and R. S. Margulies (49) of Brookhaven;

E. Z. Block, D. E. Davenport, (8), G. L. Lynn and D. C. Pound (18), and C. R. Richey (58) of Hanford; and G. McCammon (45) (61) of Oak Ridge.

Among the major contributors to the theory are E. Fermi, K. Darrow (16), Friedman, F. L. (22), P. F. Gast (23), S. Glasstone and M. C. Edlund (24), D. K. Holmes and R. V. Meghreblian (38), D. J. Hughes (40), Soodak and Campbell (64), and Weinberg, A. M., and L. C. Noderer (71).

Many refinements in measuring techniques have been made since earlier sigma pile measurements. It was quickly realized that in order to obtain very accurate values of moderator parameters, absorption by construction materials, nitrogen in graphite pores and streaming in voids, differences in density, and other factors must be taken into consideration (46) (11) (4). Techniques such as pile oscillators have provided different methods of parameter determinations (36).

V PILE DESCRIPTION

The pile is 66" x 66" x 8', a size which is sufficient for measurement of basic moderator parameters, and which was governed by space and size of blocks available.

Foil loading is accomplished by removal of foil blocks to a point where the foil hole is exposed. To facilitate the removal of blocks, and since it was necessary to use 16 1/2" blocks for the pile, foil blocks on faces A and D are provided with eye bolts and a coupling mechanism, which is shown in figures 6 and 6A. Only the first two foil blocks in a foil channel are coupled together, as this provides for foils in each level of the pile. The channel may be completely cleared by pushing the last two blocks out with a rod (figure 4).

One foil block couple was drilled with multiple foil holes along the top (figure 5) to provide for horizontal foil traverses or other possible experiments requiring multiple horizontal facilities.

One set of blocks was cut to receive probe detectors, and consists of one 32" block and two 16 1/2" blocks (figure 3). By use of these blocks in the various levels, traverses at any level may be made.

A rigid framework was placed around the pile as shown in figures 1, 1a, and 1b. This framework is primarily to hold two vertical plates in position. The backing plates have an adjustable positioning bolt and a push-rod hole for each foil channel which opens into the backing plate. By means of these bolts, the foil blocks may be returned to a reproducible position each time they are removed.

FIG. 1 ASSEMBLED PILE

SCALE 1/2" = 1'

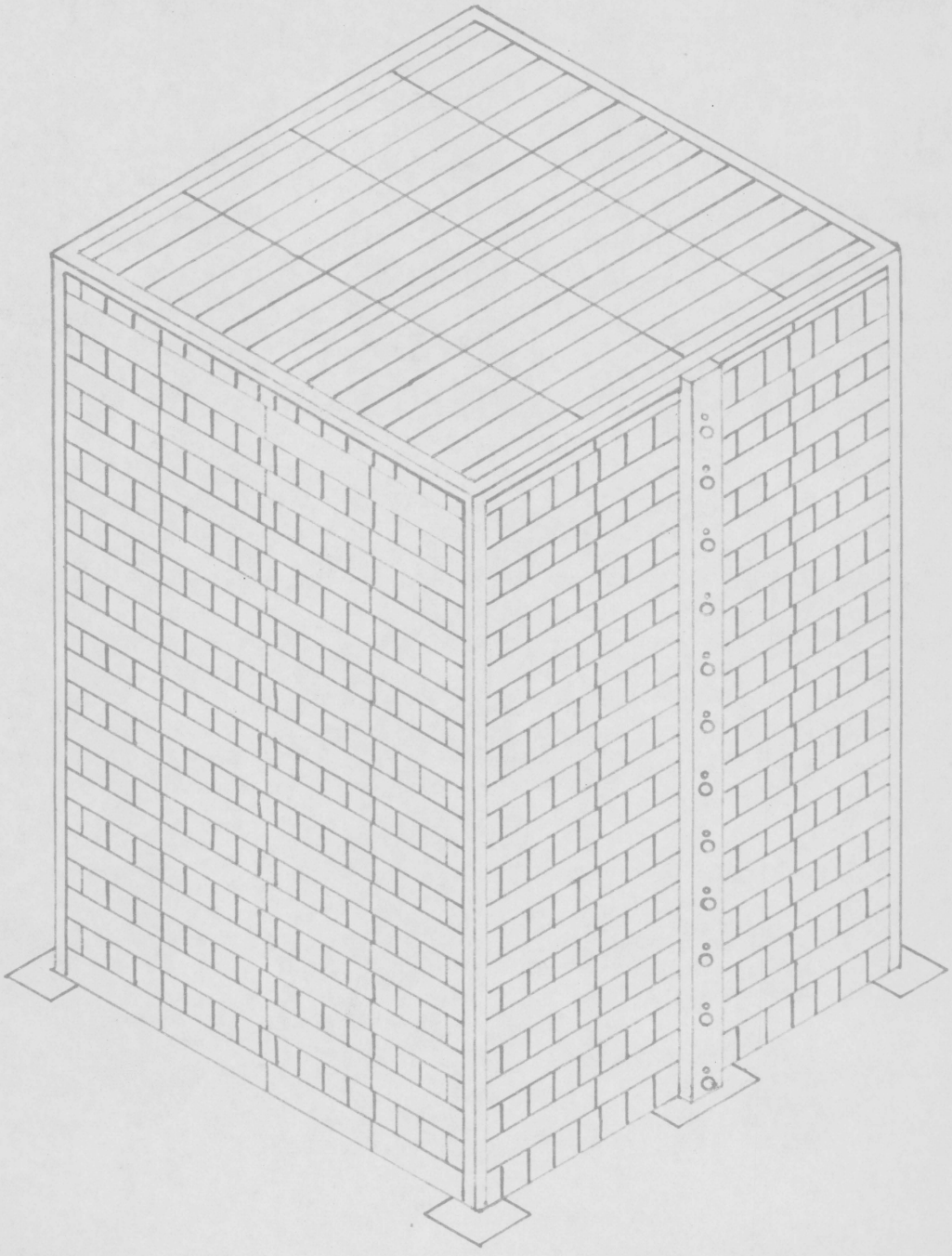

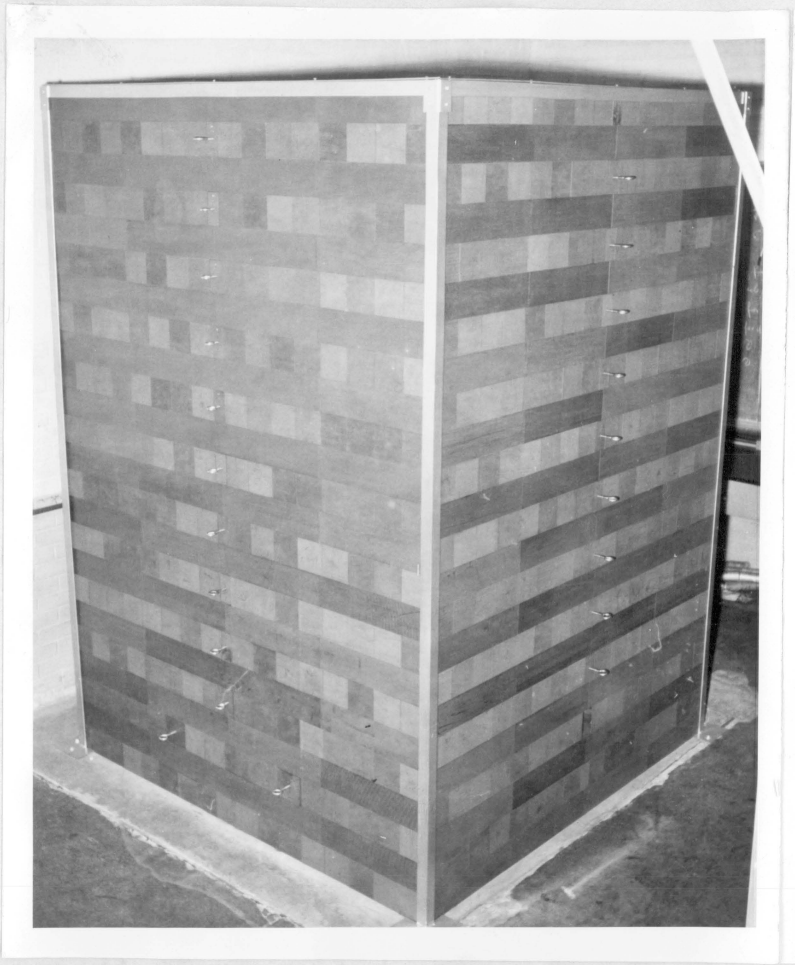

Fig. 1a

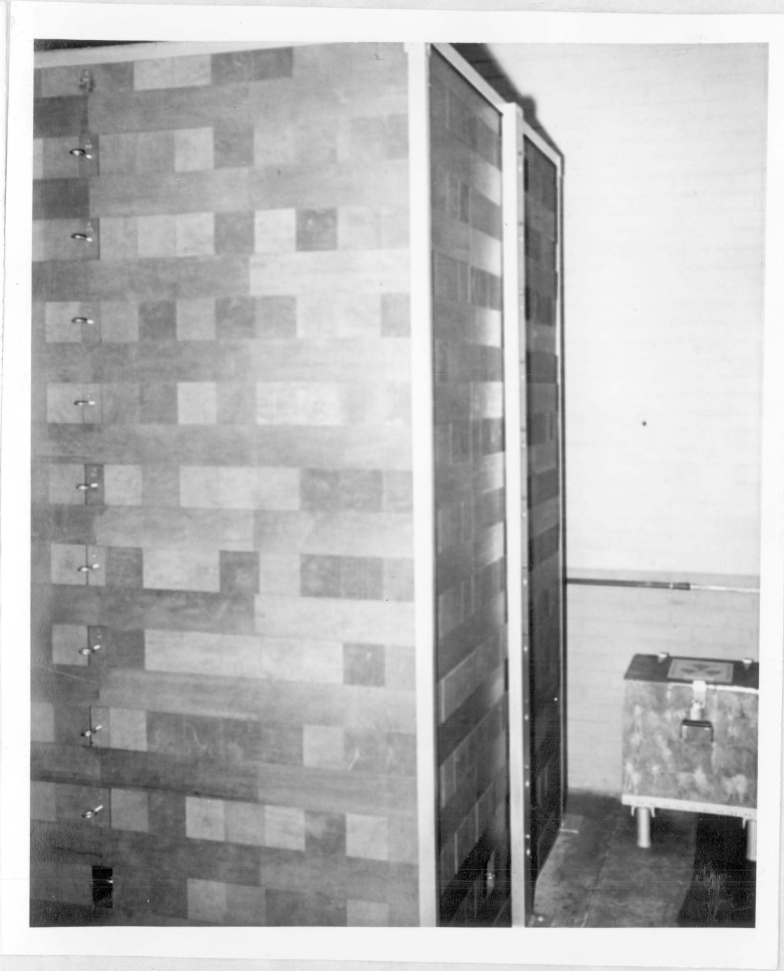

Fig. 1b

Assembled Pile

There are five possible source positions in the pile. The single central position in layer four is presently in use with the polonium-beryllium source. Four additional plutonium-beryllium sources have recently been received and will be placed in level three at distances $\pm \frac{a}{3}$ in the source blocks in this layer, where a is the extrapolated pile length. These additional sources will be used to supplement the present one, or may be placed in position to minimize harmonics.

It is planned to use the pile both as a sigma pile and a standard pile. The distinction (41) between the two is merely that the sigma pile is a large volume of moderator which was initially used to obtain the absorption cross-section (from whence comes "sigma"), while the standard pile is one of known parameters and in which the resonance and thermal flux may be calculated at points within the pile.

FIG. 2 PLAN VIEW OF SOURCE & STANDARD BLOCKS

SCALE 3/16" = 1"

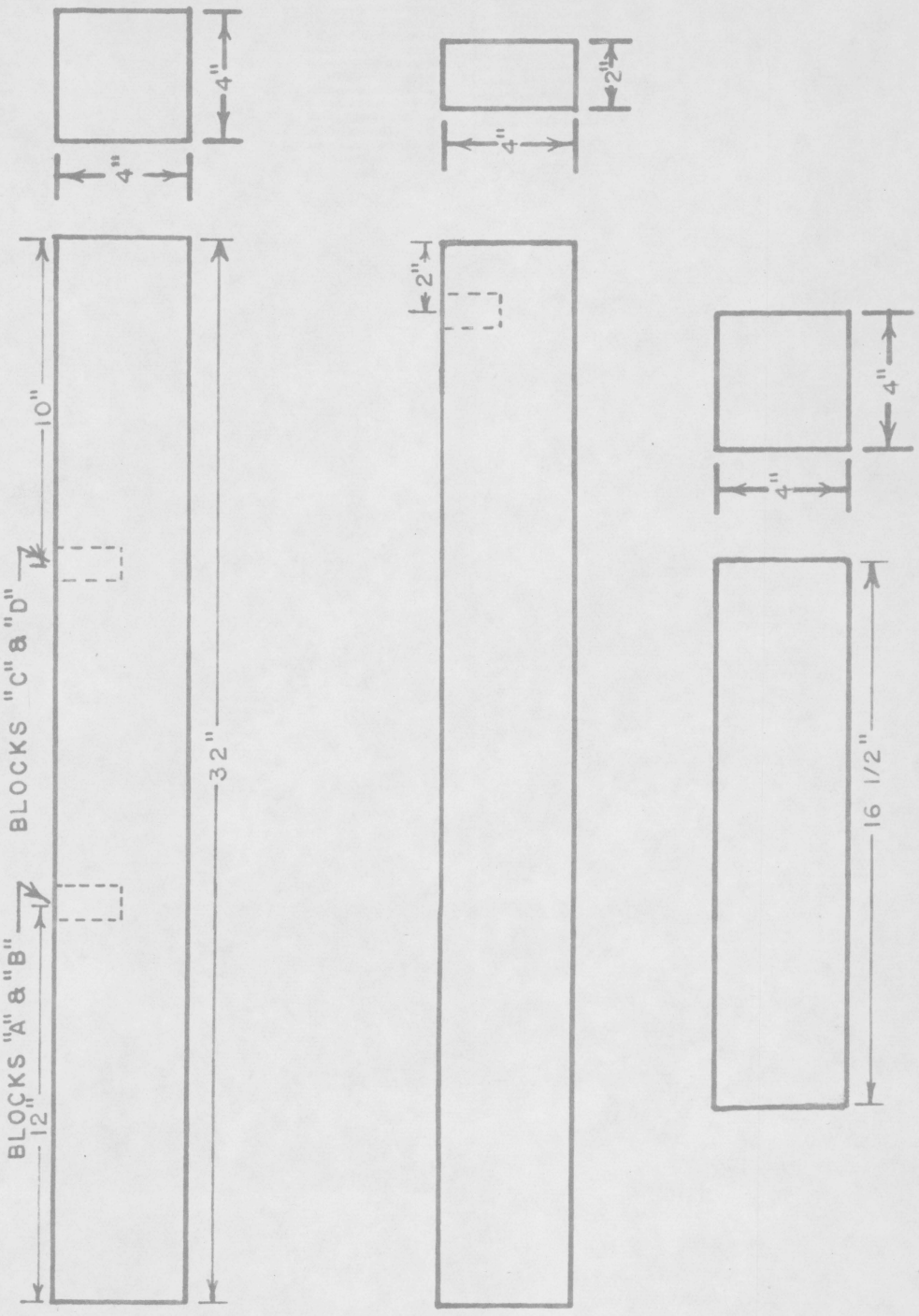

FIG. 3 PLAN VIEW OF BF_3 BLOCKS

SCALE 3/16"= 1"

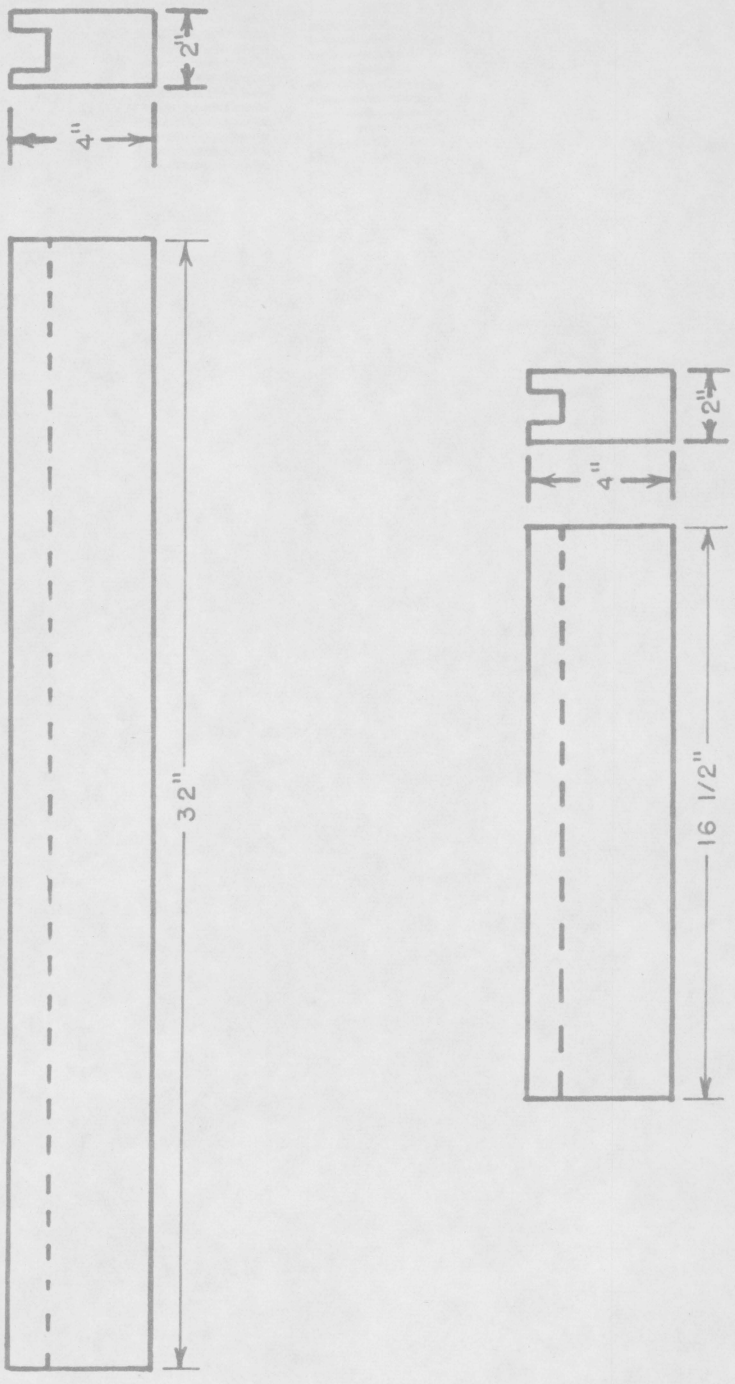

Fig. 3a Photograph of Block Types

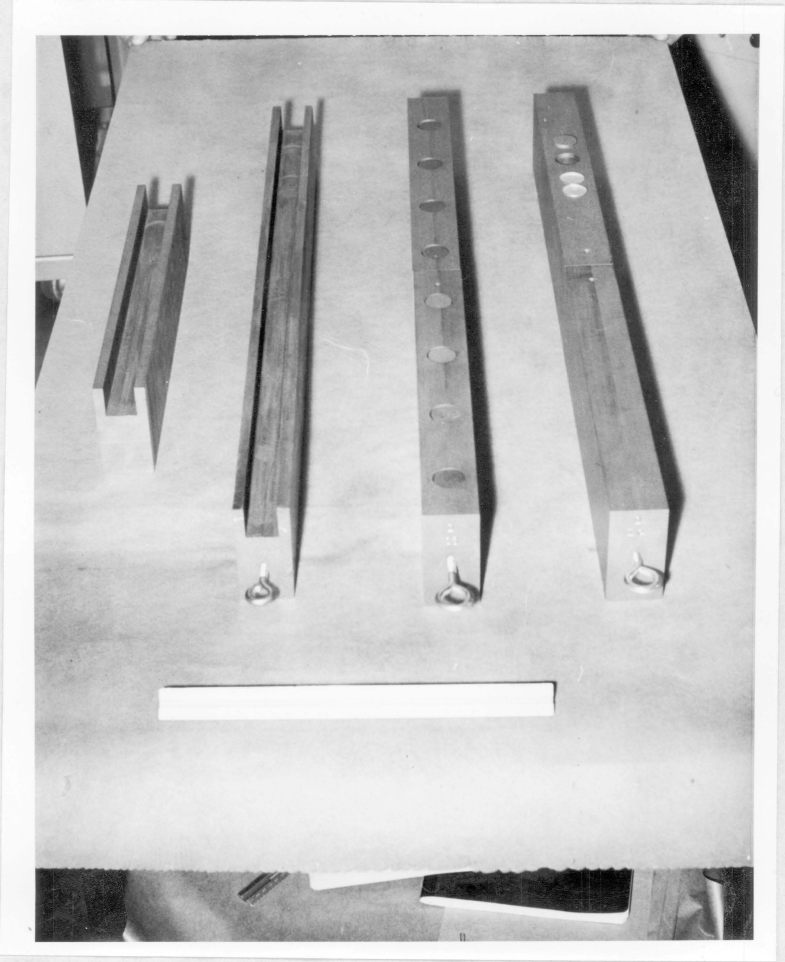

FIG. 4 PLAN VIEW OF POSITIONING MECHANISM

FULL SCALE

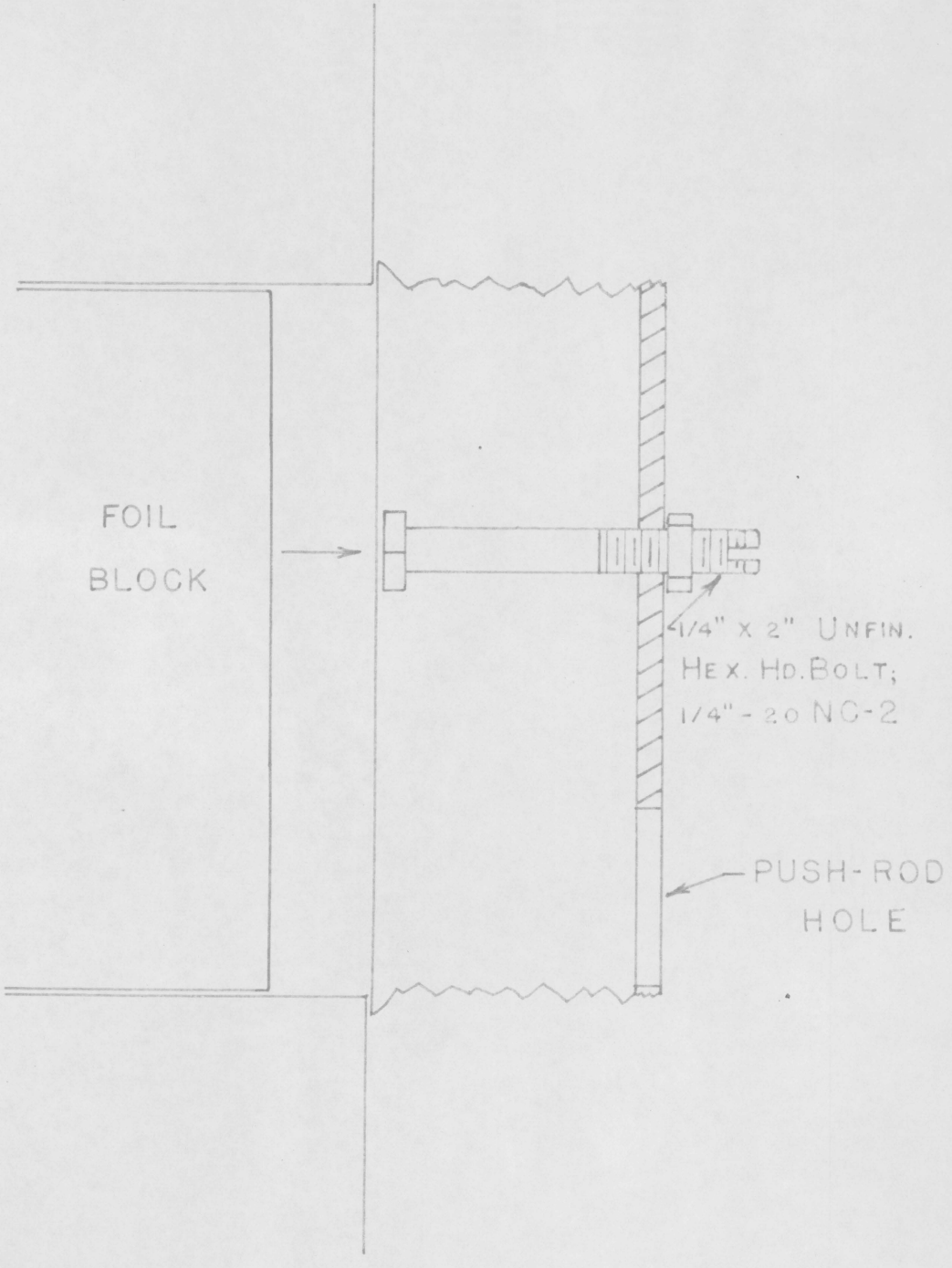

FIG. 5 PLAN VIEW OF FOIL BLOCKS

SCALE 3/16"=1"

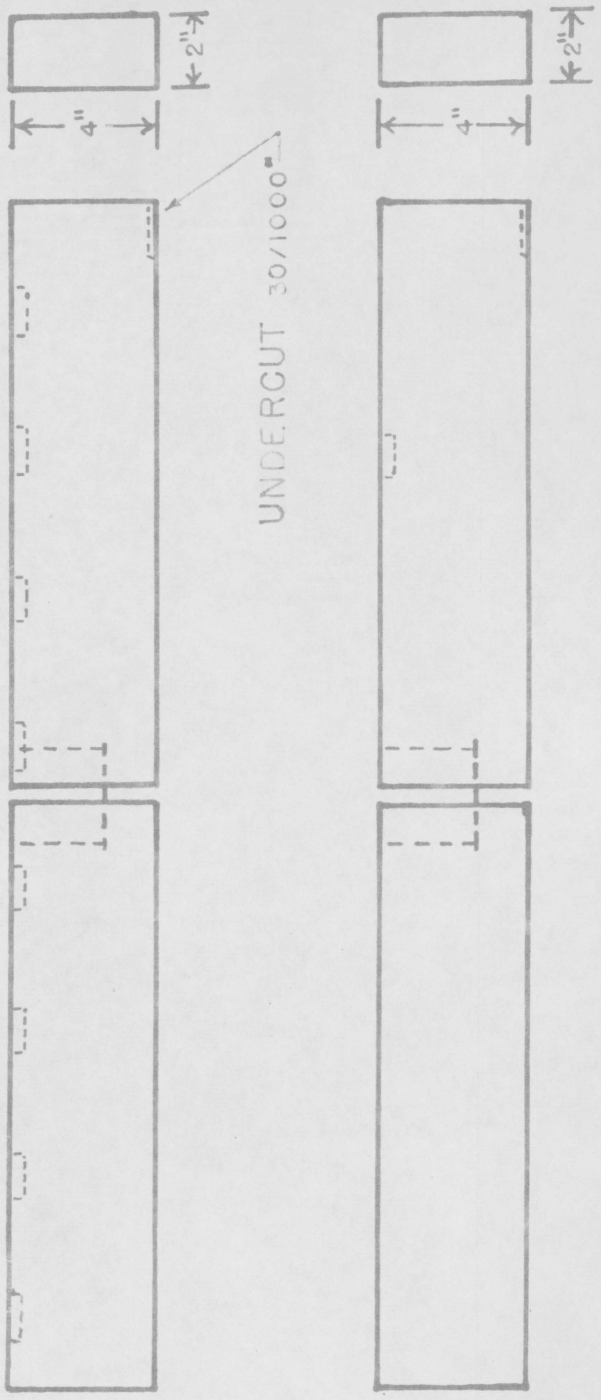

FIG.6 PLAN VIEW OF FOIL BLOCK COUPLING MECHANISM

FULL SCALE

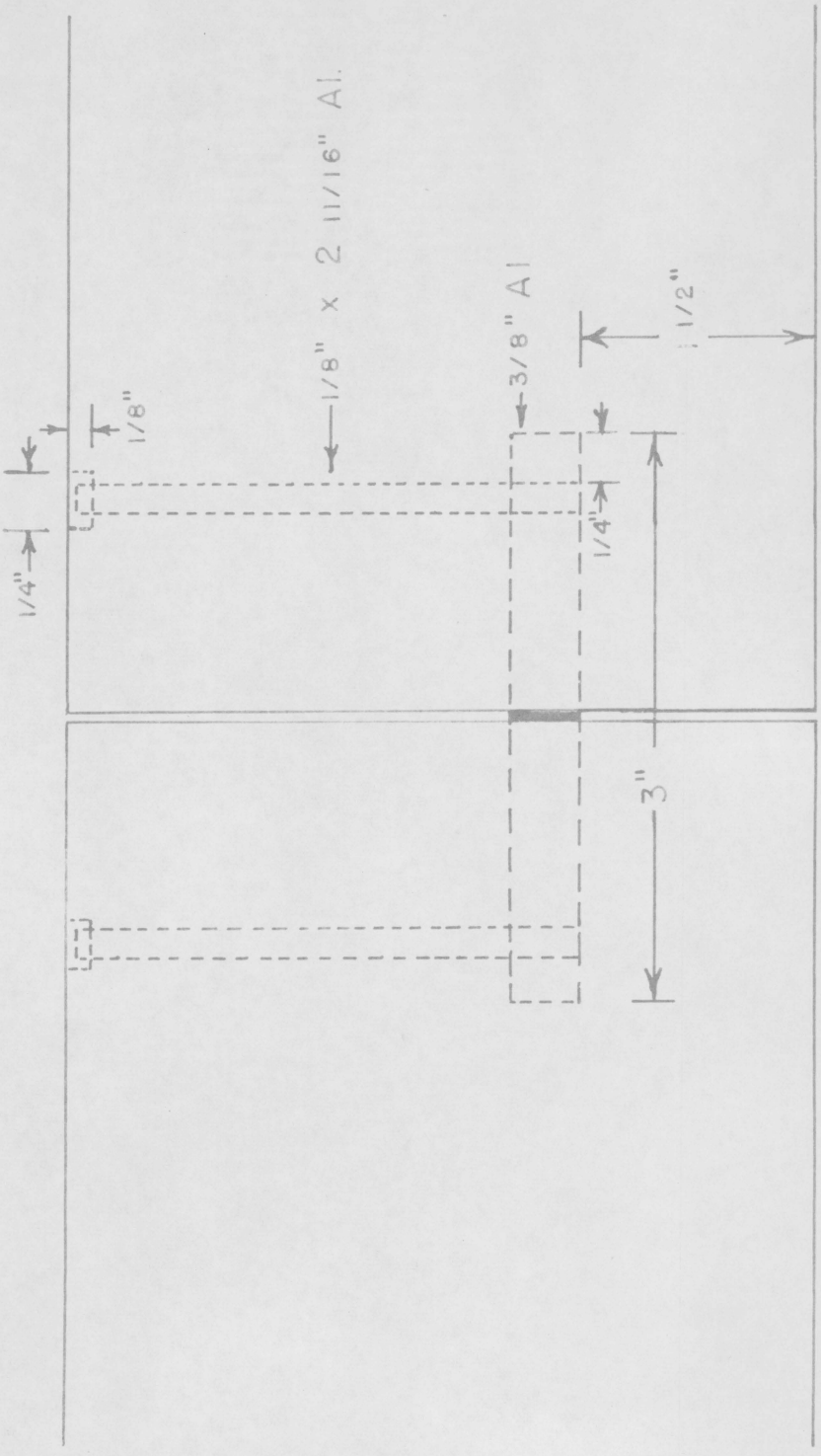

Fig. 6a Photograph of Coupling Mechanism

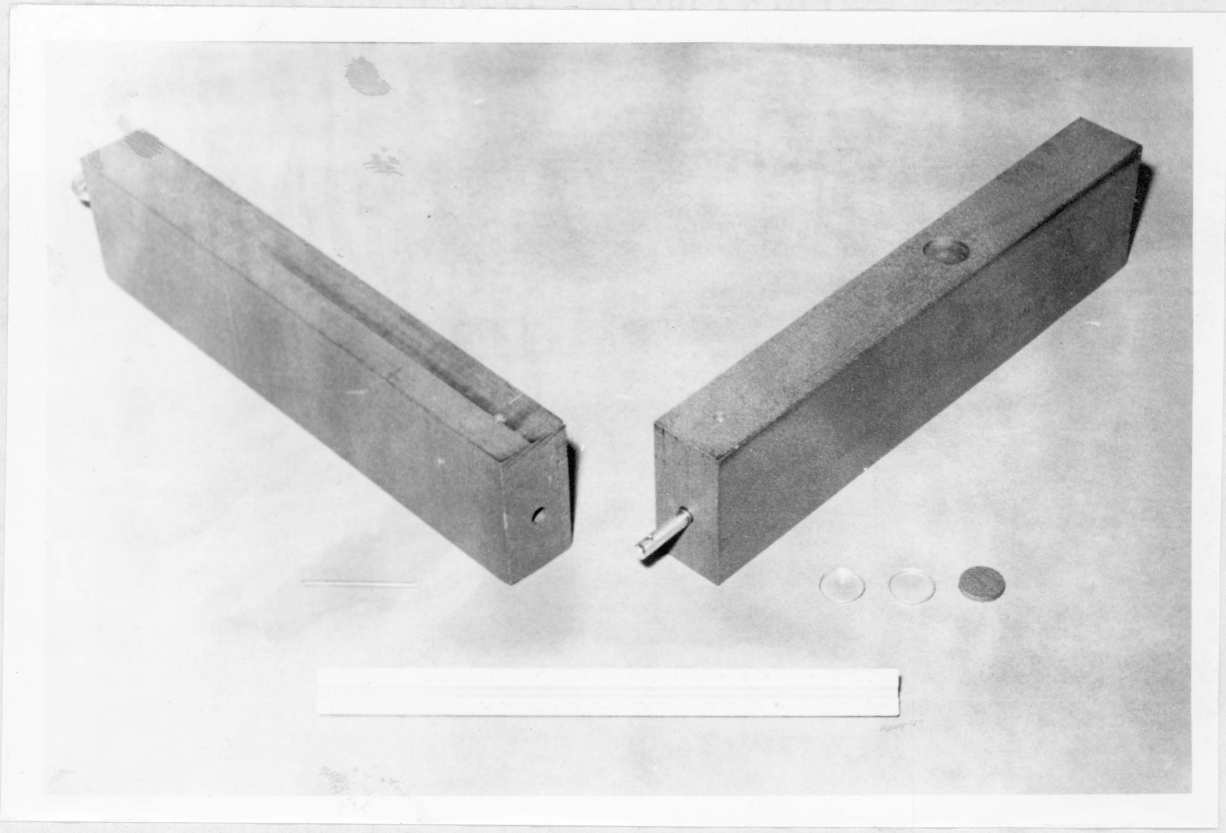

VI PILE CONSTRUCTION

Materials

The moderating material used in this pile was AGOT reactor grade graphite, obtained from National Carbon Company. This type of graphite is made from petroleum coke, which is prepared in refineries by the polymerization and distillation of volatiles from a heavy refinery oil. After further processing, the coke is crushed, screened, and mixed with a pitch binder. The plastic material so obtained is then extruded, "cooked" and purified at high temperatures in a purifying gas. The graphite bars were 16.5 $\pm$ .010" long and 4.000 $\pm$ .010 x 4.000 $\pm$ .010 inches in cross-section. Each bar was individually wrapped in paper and each skid covered with a plastic and a cardboard cover for protection of the graphite.

Metal used within the pile above the source level is confined to aluminum, which was chosen for its relatively low absorption cross-section, short-lived isotopes, and ease of machining. The aluminum is used for the specific purpose of coupling the foil blocks together, as mentioned under Pile Description.

The positioning framework is made of iron, and coated with aluminum paint. Brass bolts were used at all frame junctions to facilitate disassembly.

Eyebolts used for withdrawal of blocks are iron, nickel plated. 0.014" thick vinyl plastic is used for the dust cover. The cover is secured to the top of the metal frame-work by strips of 1" x 1/8"

steel. Brass bolts pass through the steel strips, plastic, and into the angle iron, which is tapped to receive five 10-32 bolts per side.

The base for the pile consists of a thick (about three feet) concrete block 80 x 80 inches. This base was then covered with building paper (asphalt paper sandwiched between Kraft paper).

It was decided to undercut only a few blocks before the pile was stacked. These few blocks would serve as guides for aligning the foil block channels. By laying these undercut blocks in the foil channels, and subsequently removing them after the next layer had been laid, the guide blocks were to be utilized for the stacking of the entire pile.

Machining Process

The blocks were undercut using a National heavy-duty H. S. plain milling cutter 3" x 6" x 1¼" with eight teeth. A feed of 19 inches per minute and a spindle speed of 360 rpm were used.

After undercutting, the blocks were split in two lengthwise on a "Do-all" band saw. A 3/8" buttress blade (Pitch 4, set 0.043, gauge 0.025, code YEAR) was used at a speed of approximately 1900 feet/min.

Assembly of Pile

The first two layers were stacked without incident, but as the third and fourth layers were added, it became apparent that due to the variation in block lengths, two sides of the pile would have to be slightly irregular in order to make two pile faces smooth. It was decided to have faces "A" and "D" smooth.

After stacking six layers, it was noted that because of accumulated variations in block size, it might be necessary to undercut the

permanent foil blocks more than ten thousandths. At this point, however, block variation was not considered to be a significant problem.

The stacking of the thirteenth layer indicated that these accumulated variations in blocks, even though the blocks were generally within tolerance, would cause a serious seam at at least two joints. To correct this situation, an iron "I" beam was run through the foil block hole in layer five, and a heavy auto type jack was used to raise the higher blocks in the center of side "D" just enough to replace two blocks in this region.

Replacement of these two blocks did not completely alleviate the situation, so the blocks in the right side of face "D" were unstacked down through layer two, to a depth of one to four blocks into the pile. This area was then restacked, the blocks being checked with a micrometer to obtain optimum placement.

After stacking layer fourteen, it was noted that a significant hump was forming in the foil channels which run from face "D" to face "B". This was probably caused by a slight variation in the base magnified by accumulated block variations. Blocks in the vicinity in the exposed layer were replaced with small blocks. After much consideration of various corrective measures, including restacking of the pile, a broaching operation was decided upon. A broach was made from a 14" piece of 2 x 4 inch board. A notch was cut in the top of the leading edge to receive a tool steel cutting edge. It was found that the cutting edge had to be sharp and hollow-ground for satisfactory service. Once this was established, the broach needed no subsequent

sharpening or modification at any time. The broach was pushed through by a wooden rod or wooden blocks, depending on the placement and size of the channel. The closeness of an adjoining room wall made the operation very time-consuming when working on channels running from side "A" to side "C". A Black and Decker industrial vacuum cleaner was used to remove graphite chips from the channels.

Stacking was resumed after twelve layers had been broached. The upper 1/4 - 1/3 of the pile was laid more slowly, since every block was measured with a micrometer to insure its best placement.

It was noted that lighter broaching cuts were required in the upper portion of the pile than in the lower portion. In all cases, blocks which were undercut ten thousandths were able to pass through the length of each foil channel after broaching.

Forty-six 16 1/2 x 4 x 4 inch blocks were undercut ten-thousandths of an inch and split lengthwise.

Inserting the foil blocks in the channels is like inserting a key in a keyway. The bottom of the blocks project downward into the broached area of the next lower channel, partially impeding movement of blocks in the lower channels at the center of the pile. Since the source block is also keyed, the unauthorized removal of the source is difficult. It is noted here that in general, only the top of each channel was broached. To facilitate the removal of foil blocks, the two center blocks in each foil channel were undercut on the bottom 0.030 inch for a distance of one inch from the end which was to be in the center of the pile. Thus, when the complement of four foil blocks

is inserted in the channel, there is sufficient clearance for motion of the blocks in the next lower channel.

Five thirty-two inch blocks were taken from the exponential pile and exchanged for short blocks since all blocks obtained for the sigma pile were 16 1/2" long. The long blocks were milled to reduce twist acquired in manufacture, probably during the extruding operation. After squaring, they were then undercut in preparation for use as source blocks. One of these was split; one half was to serve as a source block, the other as a probe detector block in conjunction with two short blocks.

Thirty-eight of the foil blocks were coupled in two's as shown in figures 5 and 6. The outer block of each couple was drilled, tapped, and fitted with an eye bolt to facilitate removal. Before placement in the pile, the inner block of each couple was drilled as shown in figure 5 to receive indium foils with or without cadmium covers. Foil holes not in use are filled with graphite washers to decrease flux disturbances.

The 32 x 2 x 4 inch block and two 16 1/2 x 2 x 4 inch blocks were slotted approximately 1 1/8 x 1 1/8 inch for use with a probe detector. An eye bolt was installed on the 32" block.

The positioning framework was made from 1 1/2 x 1 1/2 inch angle iron and 4" x 1 1/2" channel iron. It was fastened together by welding and by brass bolts. Attachment to the floor was by means of 1/4" - 20 expansive screw anchors. The iron was cleaned with an electric portable wire brush and painted with aluminum paint.

VII THEORY

Diffusion Length (25)

The theoretical balance equation for a nuclear chain reactor is given by

$$\text{Production} - \text{Leakage} - \text{Absorption} = \frac{\partial n}{\partial t}$$

where $\frac{\partial n}{\partial t}$ is the time rate of change of the neutron density. For steady state operations, this reduces to

$$\text{Production} = \text{Leakage} + \text{Absorption}.$$

In diffusion systems, it is found that the diffusing substance tends to go from regions of high density to regions of low density. It is assumed that neutrons also follow this theory and that Fick's law in the simple form $J(x) = -D\nabla\phi$ is applicable to neutrons, where

J = net number of neutrons flowing per unit area normal to the direction of flow, per unit time.

D = diffusion coefficient for flux.

ϕ = neutron flux (nv)

The net rate of outflow of neutrons per unit volume is equal to the divergence of the vector J. So the neutron leakage per unit volume per second is given by

$$\text{div } J = -\text{div } D\nabla\phi.$$

$$= -D\nabla^2\phi$$

The absorption rate (neutrons absorbed per cm^3 per second) is represented by $\sum a\phi$, where $\sum a$ is the macroscopic absorption cross section of the medium.

The production may be represented initially by a source term, S (neutrons per cm^3 per second).

The balance equation is now given by

$$Dv^2\phi - \Sigma_a\phi + S = \frac{\partial n}{\partial t}$$

and is called the diffusion equation. Its limitations are that it is applicable only to monoenergetic neutrons, at distances greater than two or three mean free paths from strong sources, absorbers, or boundaries between dissimilar materials.

If $\frac{\partial n}{\partial t}$ is zero, and S is zero except at the source (point, line, or plane source), the diffusion equation becomes

$$Dv^2\phi - \Sigma_a\Phi = 0.$$

If a constant, k, is introduced such that

$$k \equiv \frac{\Sigma_a}{D},$$

then the diffusion equation is

$$\nabla^2\phi - k^2\phi = 0.$$

General solutions of the above type equation may be obtained by standard methods, and boundary conditions applied to suit the particular geometry in question.

For a point source which releases one neutron per second in an infinite homogeneous diffusion medium, if ∇^2 is expressed in spherical coordinates

$$\nabla^2 \equiv \frac{\partial^2}{\partial r^2} + \frac{2}{r} \cdot \frac{\partial}{\partial r} + \frac{1}{r^2 \sin\theta} \cdot \frac{\partial}{\partial \theta} \left(\sin\theta \frac{\partial}{\partial \theta}\right) + \frac{1}{r^2 \sin^2\theta} \cdot \frac{\partial^2}{\partial \phi^2}$$

The diffusion equation is then:

$$\frac{d^2\phi}{dr^2} + \frac{2}{r} \cdot \frac{d\phi}{dr} - k^2\phi = 0, r \neq 0$$

in spherical coordinates, if the coordinate system is chosen with its origin at the point source, where r is the distance from the source.

The boundary conditions are:

(1) $\phi < \infty$ for $r > o$.

(2) The total number of neutrons passing through the surface of a sphere equals the source strength as r approaches zero,

or $\lim_{r \to 0} 4\pi r^2 J = 1$.

If $\phi \equiv u/r$, the equation may be solved:

$$\frac{d^2\left(\frac{u}{r}\right)}{r^2} + \frac{2}{r}\frac{d\left(\frac{u}{r}\right)}{dr} - k^2\left(\frac{u}{r}\right) = 0$$

reduces to

$$\frac{d^2u}{dr^2} - k^2u = 0$$

or

$$(D^2-k^2)u = 0$$

$$D^2 = k^2,$$

$$D = \pm k$$

But since k is positive by definition,

$$D = +k$$

and $u = A e^{-kr} + Ce^{kr}$

so $\phi = Ae\frac{-kr}{r} + C\frac{e^{kr}}{r}$.

The first boundary condition requires that $C \equiv 0$.

The current density (J) at r is

$$J = -D\frac{d\phi}{dr} \text{ or } -D\frac{d}{dr}\left(\frac{Ae^{-kr}}{r}\right) \text{ or } DAe^{-kr}\left(\frac{Kr+1}{r^2}\right).$$

Applying this to the source condition,

$$\lim_{r \to 0} 4\pi r^2 J = \lim_{r \to 0} 4\pi DAe^{-kr}(Kr + 1) = 1.$$

So $A = \frac{1}{4\pi D}$

Therefore,

$$\phi = \frac{e^{-kr}}{4\pi Dr}$$

Since the study of thermal neutrons is usually of most interest in many types of reactors, the preceding treatment of monoenergetic neutrons is applied to a thermal system. This is a reasonable approximation, since in weakly absorbing media, thermal neutrons behave in an approximately monoenergetic fashion with properly averaged absorption cross section and mean free path. (26)

The mean square distance, $\overline{r^2}$, which a thermal neutron travels from its source to where it is absorbed may be determined by consideration of a point source, with a flux of ϕ neutrons per cm^2 per second at a distance r. The absorption rate is $\Sigma a \ \phi$ per cm^3 per second; for a spherical shell of volume $4\pi r^2 dr$, the absorption rate is $4\pi r^2 dr \Sigma a \phi$. The mean square distance to absorption is then

$$\overline{r^2} = \frac{\int_0^\infty r^2 (4\pi r^2 \Sigma a \phi) dr}{\int_0^\infty 4\pi r^2 \Sigma a \phi dr}$$

from the definition of the r.m.s. value of $y = f(x)$ over the interval $x = a$ to $x = b$. (57)

Substituting $\phi = e^{-kr}/4\pi Dr$,

$$\overline{r^2} = \frac{\int_0^\infty r^3 e^{-kr} dr}{\int_0^\infty r e^{-kr} dr} = \frac{\frac{6}{k^4}}{\frac{1}{k^2}} = \frac{6}{k^2}$$

If the diffusion length, L, in a medium be defined by $L \equiv 1/k^2$, then

$$\overline{r^2} = 6L^2$$

and $\phi = Ae^{-x/L}$, or L is equivalent to the relaxation length.

Since the above treatment is not applicable to actual conditions because of leakage which occurs in finite systems, the diffusion (or wave) equation must be solved as a boundary value problem.

The problem is stated:

$$\nabla^2\phi - k^2\phi = 0,$$

with the boundary conditions:

(1) ϕ is everywhere finite and non-negative.

(2) $\phi = 0$ at the extrapolated boundaries.

(3) The number of neutrons flowing out of the plane $z = 0$ per cm^2 per sec in each mode must equal the number produced in that mode by the source.

This is solved for positive values of z, and appears as

$$\frac{\partial^2\phi}{\partial x^2} + \frac{\partial^2\phi}{\partial y^2} + \frac{\partial^2\phi}{\partial z^2} - k^2\phi = 0.$$

By assuming separation of variables,

$\phi = X(x)Y(y)Z(z)$; this becomes

$$\frac{1}{X} \cdot \frac{d^2X}{dx^2} + \frac{1}{Y}\frac{d^2Y}{dy^2} - \frac{1}{Z} \cdot \frac{d^2Z}{dz^2} - k^2 = 0.$$

Since the sum of the first three terms must equal a constant, k^2, and since they are independent functions, we may write:

$$\frac{1}{X} \cdot \frac{d^2X}{dx^2} = -\alpha^2,$$

$$\frac{1}{Y} \cdot \frac{d^2Y}{dy^2} = -\beta^2, \text{ and}$$

$$\frac{1}{Z} \cdot \frac{d^2Z}{dz^2} = \gamma^2.$$

It should be noted that $-\alpha^2 - \beta^2 + \gamma^2 = k^2$

The signs given α and β are to insure sine and cosine solution, since it may be seen from a flux distribution plot (27) that hyperbolic functions (and also the sine functions) are not permissable solutions because of boundary conditions (1) and (2).

Therefore,

$$X = A \cos kx$$

is the only permissable solution, and α^2 and β^2 must be preceded by a minus sign, if they are to be positive. If γ^2 is also positive, it must have a positive sign since k^2 is a real number greater than zero.

So the above solution is written as

$$X = A \cos \alpha x.$$

In order to satisfy boundary condition (2),

$$\alpha = \frac{n\pi}{a}, \text{ where } n = 1, 3, 5, \ldots.$$

so that when x is equal to a/2, then

$$X\left(\frac{a}{2}\right) = A \cos \frac{n\pi}{2} = 0.$$

The solution may be generalized, and a like solution obtained for Y, as

$$X_m = A_m \cos \frac{m\pi x}{a} \qquad m = 1, 3, 5, \ldots$$

and

$$Y_n = B_n \cos \frac{n\pi y}{b} \qquad n = 1, 3, 5, \ldots$$

Solving for Z, since γ^2 is positive, the solution will be of the hyperbolic form

$$Z = C_1 \cosh \gamma z + C_2 \sinh \gamma z$$

C_2 is evaluated from boundary condition (2), and

$$Z = \frac{C_1}{\sinh \gamma c} (\sinh \gamma c \cosh \gamma z - \cosh \gamma c \sinh \gamma z)$$

$$\text{or } C_3 \sinh (c-z), \text{ or } \frac{C_3}{2}\left[e^{\gamma(c-z)} - e^{-\gamma(c-z)}\right]$$

$$\text{or } C\, e^{-\gamma z}\left[1 - e^{-2\gamma(c-z)}\right].$$

If the z dimension is very long, then

$$Z = C\, e^{-\gamma z}.$$

In view of the series of possible values of α and β, γ and z may be expressed as

$$\gamma^2_{mn} = k^2 + \left(\frac{m\pi}{a}\right)^2 + \left(\frac{n\pi}{b}\right)^2,$$

$$\text{and } Z = C_{mn}\, e^{-\gamma_{mn} z}$$

Since the wave equation is linear, any sum of the products of X, Y, and Z will be a solution, and

$$\phi = \sum_{m=1}^{\infty} \sum_{n=1}^{\infty} A_{mn} \cos \frac{m\pi x}{a} \cos \frac{n\pi y}{b}\, e^{-\gamma_{mn} z}.$$

The source condition is introduced to determine A_{mn}. A thermal point source, at the origin, emitting S neutrons per second, may be defined in terms of the Dirac delta function as $s\,\delta(x,y)$ at $z = 0$. Expanding the source in a series of orthogonal functions,

$$S\delta(x,y) = \sum_{m=1}^{\infty} \sum_{n=1}^{\infty} S_{mn} \cos \frac{m\pi x}{a} \cos \frac{n\pi y}{b};$$

$$S \int_{-a/2}^{a/2} \int_{-b/2}^{b/2} \delta(x,y) \cos \frac{k\pi x}{a} \cos \frac{l\pi y}{b} dxdy =$$

$$\int_{-a/2}^{a/2} \int_{-b/2}^{b/2} S_{mn} \cos \frac{m\pi x}{a} \cos \frac{n\pi y}{b} \cos \frac{k\pi x}{a} \cos \frac{l\pi y}{b} dxdy$$

$$S \int_{-a/2}^{a/2} \int_{-b/2}^{b/2} \delta(x,y) \cos \frac{m x}{a} \cos \frac{n y}{b} dxdy =$$

$$\int_{-a/2}^{a/2} \int_{-b/2}^{b/2} S_{mn} \cos \frac{m\pi x}{a} \cos \frac{k\pi x}{a} \cos \frac{n\pi y}{b} \cos \frac{l\pi y}{b} dxdy$$

Since the functions are orthogonal in the intervals -a/2 to a/2 and -b/2 to b/2, all terms not having m = k or n = l will be zero. Thus,

$$S \int_{-a/2}^{a/2} \int_{-b/2}^{b/2} \delta(x,y) \cos \frac{m\pi x}{a} \cos \frac{n\pi y}{b} dxdy =$$

$$S_{mn} \int_{-a/2}^{a/2} \cos^2 \frac{m\pi x}{a} dx \int_{-b/2}^{b/2} \cos^2 \frac{n\pi y}{b} dy$$

From the definition of the Dirac delta function, i.e. it has the value of zero everywhere except at x = 0 and y = o, at which point it has the value

$$\int_{-\infty}^{\infty}\int_{-\infty}^{\infty} \delta(x,y)\,dxdy = 1.$$

So the left side of the equation becomes S at the source. The right side becomes

$$S_{mn}\left[\left(\frac{x}{2} + \sin\frac{2m\pi x}{a}\right)_{-a/2}^{a/2} \cdot \left(\frac{y}{2} - \sin\frac{2m\pi y}{a}\right)_{-b/2}^{b/2}\right]$$

$$\text{or } S_{mn}\left[\left(\frac{a}{4} + \frac{a}{4}\right)\left(\frac{b}{4} + \frac{b}{4}\right)\right], \text{ or}$$

$$S_{mn}\left[\frac{ab}{4}\right].$$

Hence, $S_{mn} = \frac{4S}{ab}$

To determine A_{mn}, use is made of the current density.

$$J_{mn} \text{ at } z = 0 = -D\frac{\partial\phi_{mn}}{\partial z} = D\gamma_{mn} A_{mn} \cos\frac{m\pi x}{a} \cos\frac{n\pi y}{b} = \frac{S_{mn}}{2}$$

since only the positive z direction is being considered.

Thus $J_{mn} = 1/2\left(\frac{4S}{ab}\right)\cos\frac{m\pi x}{a}\cos\frac{n\pi y}{b}$,

and $A_{mn} = \frac{2S}{abD\gamma_{mn}}$,

By a harmonic analysis (44) of the flux in the positive z direction, it is seen that beyond two diffusion lengths from the source, the harmonic flux contribution is relatively small.

Thus, under these conditions,

$$\phi(z) = (\text{const.})\ x\left(e^{-\gamma_{11} z}\right),$$

and $$\frac{d \ln \phi(z)}{dz} = -\gamma_{11},$$

so that a plot of ln saturated activity versus z will have a slope of $-\gamma_{11}$.

Since m and n are unity,

$$k^2 = \gamma_{11}^2 - \left(\frac{\pi}{a}\right)^2 - \left(\frac{\pi}{b}\right)^2 ,$$

By obtaining γ_{11} experimentally, k^2 may be found, and therefore L, since $L = 1/k$.

The final expression for the diffusion length is then

$$L = \sqrt{\frac{1}{\gamma_{11}^2 - \left(\frac{\pi}{a}\right)^2 - \left(\frac{\pi}{b}\right)^2}}$$

$$L = \left[\gamma_{11}^2 - \left(\frac{\pi}{a}\right)^2 - \left(\frac{\pi}{b}\right)^2\right]^{-1/2}$$

where a = extrapolated pile length

b = extrapolated pile width.

Fermi Age (29)

The Fermi Age model assumes a continuous slowing down of the neutrons. This assumption is valid for all except the lightest elements, to which a great part or all of the neutron energy may be lost in a single collision.

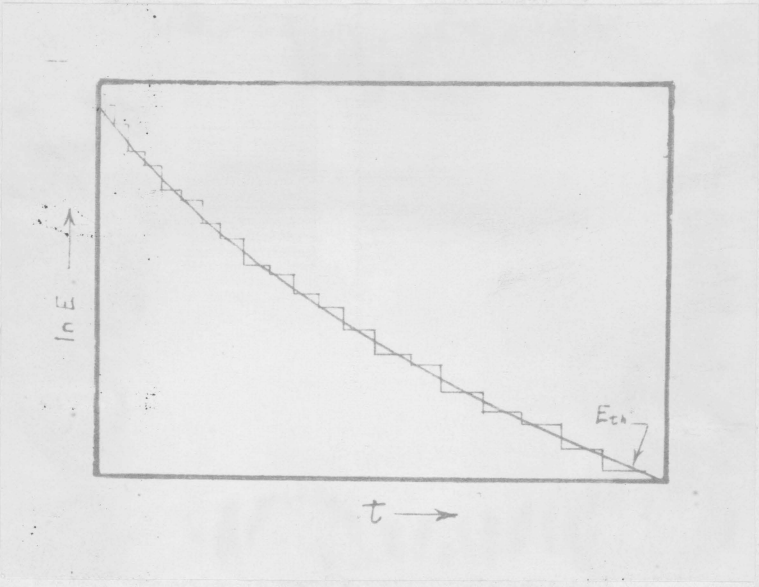

The smooth curve is the theoretical approximation, while the actual slowing down is done stepwise. A further assumption is that all neutrons have diffused for a time t, after leaving their source, and have the same lethargy, or logarithmic energy decrement. Lethargy is defined by $u \equiv \ln \frac{E_o}{E}$, where E_o is the initial energy of the source neutron produced by fission.

An average logarithmic energy decrement per collision, ξ, is defined by

$$\xi \equiv \overline{\ln \frac{E_1}{E_2}} = \frac{\int_{E_1}^{\alpha E_1} \ln \frac{E_1}{E_2}\, p(E_2)dE_2}{\int_{E_1}^{\alpha E_1} p(E_2)dE_2},$$

where E_1 is the energy of the neutron before and E_2 that after a collision, and where $p(E_2)dE_2$ is the probability that after scattering a neutron with initial energy E_1 will have an energy in the interval E_2 to $E_2 + dE_2$. The integration is performed over all possible values

of the energy after collision, from the minimum, equal to αE_1, to the maximum E_1.

The ratio of the neutron energy after collision to that before collision is shown to be (24).

$$\frac{E_2}{E_1} = \frac{v_2^2}{v_1^2} = \frac{v_m^2 + v_a^2 + 2v_m v_a \cos\theta}{v_1^2}$$

where v_m = speed of the center of mass in the laboratory system.

v_1 = speed of the neutron in the laboratory system.

v_a = speed of the neutron after collision in the center of mass system.

v_b = speed of the nucleus after collision in the center of mass system.

v_m is given by $\frac{v_1}{A + 1}$

From the conservation of energy, assuming elastic scattering, since

$$v_1 - v_m = \frac{A v_1}{A + 1}$$

then $$\frac{1}{2}\left(\frac{Av_1}{A + 1}\right)^2 + \frac{1}{2}\left(\frac{v_1}{A + 1}\right)^2 = \frac{1}{2} v_a^2 + \frac{1}{2} A v_b^2.$$

from conservation of momentum,

$$v_a = A v_b.$$

Thus,

$$\frac{E_2}{E_1} = \frac{v_2^2}{v_1^2} = \frac{A^2 + 2A\cos\theta + 1}{(A + 1)^2}$$

A function α is defined by

$$\alpha \equiv \left(\frac{A - 1}{A + 1}\right)^2$$

The maximum value of E_2/E_1, which represents the minimum loss of energy, is unity, or $E_{max} = E_1$. The maximum loss of energy is represented by the minimum value of $E_2/E_1 = \alpha$. Therefore, ξ is defined by integration over all possible energy decrements, from E_1 to αE_1.

$p(E_2)dE_2$ may be related to $p(\theta)d\theta$, the probability that a neutron will be scattered into an element of solid angle, $d\Omega$, corresponding to a conical element lying between the scattering angles θ and $\theta + d\theta$ in the center of mass system, by

$$p(E_2)dE_2 = p(\theta)\frac{d\theta}{dE_2}\,dE_2.$$

But $p(\theta)d\theta = \frac{d\Omega}{4\pi} = \frac{2\pi \sin\theta\, d\theta}{4\pi} = 1/2 \sin\theta\, d\theta.$

From the definition of α,

$$\frac{E_2}{E_1} = 1/2\left[(1 + \alpha) + (1 - \alpha)\cos\theta\right]$$

and so $$\frac{d\theta}{dE_2} = -\frac{2}{E_1 (1 - \alpha)\sin\theta}$$

Thus, $$p(E_2)dE_2 = -\frac{dE_2}{E_1 (1 - \alpha)}$$

$$\int_{E_1}^{\alpha E_1} p(E_2)dE_2 = -\frac{1}{E_1 (1 - \alpha)}\int_{E_1}^{\alpha E_1} dE_2 = 1.$$

ξ now becomes

$$= -\int_{E_1}^{\alpha E_1} \ln \frac{E_1}{E_2} \cdot \frac{dE_2}{E_1 (1 - \alpha)} .$$

If $x \equiv \frac{E_2}{E_1}$, and $dx = \frac{dE_2}{E_1}$,

$$\xi = \frac{1}{1 - \alpha} \int_1^{\alpha} \ln x \, dx$$

$$= 1 + \frac{\alpha}{1 - \alpha} \ln \alpha .$$

ξ may also be represented as

$$\xi = 1 + \frac{(A - 1)^2}{2A} \ln \frac{A - 1}{A + 1} .$$

For $A > 10$,

$$\xi = \frac{2}{A + 2/3} .$$

Returning to the derivation of the Fermi Age equation, if, after time t, all the neutrons have velocity v, and since λ_s is the scattering mean free path, the number of collisions a neutron undergoes in dt will be vdt/λ_s. The decrease in ln E will be found by the product of ξ, the average logarithmic energy change per collision, and the number of collisions in dt, or

$$-d \ln E = \frac{\xi v}{\lambda_s} dt.$$

Since -d ln E is equivalent to du,

$$du = \frac{\xi v}{\lambda_s} dt$$

The assumption is also made that there is no absorption lose of neutrons.

As previously shown, the neutron leakage per unit volume per second is

$$\text{div } J = -Dv^2\phi,$$

and since $\phi = nv$, the leakage, without absorption, is given by

$$Dvv^2n(r,t) = \frac{\partial n(r,t)}{\partial t},$$

$n(r,t)$ is defined as the neutron density per unit time interval, so $n(r,t)\,dt$ is the number of neutrons per cm^3 which have diffused between t and t + dt.

Since $n(r,u)du = n(r,t)dt$,

$$n(r,t) = n(r,u)\frac{\partial u}{\partial t} = n(r,u)\frac{\xi v}{\lambda s}.$$

Since $\frac{\partial n(r,t)}{\partial t}$ may be written as $\frac{\partial u}{\partial t}\frac{\partial n}{\partial u}(r,t)$,

and $du = \frac{\xi v}{\lambda s}\,dt$,

$$\frac{\partial n(r,t)}{\partial t} = \frac{\xi v}{\lambda s} \cdot \frac{\partial n(r,t)}{\partial u}$$

$$\text{or} \qquad = \frac{\xi v}{\lambda s} \cdot \frac{\partial}{\partial u}\left[\frac{\xi v}{\lambda s} \cdot n(r,u)\right].$$

Upon making this substitution,

$$Dvv^2n(r,t) = \frac{\partial n(r,t)}{\partial t}, \text{ becomes}$$

$$Dvv^2\left[\frac{\xi v}{\lambda s}\,n(r,u)\right] = \frac{\xi v}{\lambda s} \cdot \frac{\partial}{\partial u}\left[\frac{\xi v}{\lambda s}\,n(r,u)\right].$$

or $$D\nabla^2\left[\xi\Sigma_s\phi(r,u)\right] = \xi\Sigma_s \frac{\partial}{\partial u}\left[\xi\,\Sigma_s\,\phi\,(r,u)\right].$$

One form of the slowing down density, q (the number of neutrons per unit volume per unit time slowed down past a given energy), is given (24) by

$$q = \xi\Sigma_s\,\phi(u).$$

Using this relationship, the above equation becomes

$$D\nabla^2 q = \xi\,\Sigma_s\,\frac{\partial q}{\partial u}\,.$$

If a new variable, τ, is defined as

$$\tau\,(u) \equiv \int_0^u \frac{D}{\xi\Sigma_s}\,du,$$

The equation reduces to

$$\nabla^2 q = \frac{\partial q}{\partial \tau} \quad \text{(Fermi Age equation)}.$$

Since $du = -dE/E$,

$$\tau = \int_E^{E_o} \frac{D}{\xi\,\Sigma_s}\,\cdot\,\frac{dE}{E}\,.$$

The Fermi Age Equation may be solved first for a plane source of fast monognergetic neutrons in an infinite medium, and this result used to solve the case of a point source of fast monoenergetic neutrons in an infinite medium, which solution is used as the basis for experimental determinations of Fermi Age in many cases.

The relationship between the slowing down density for neutrons of

a specific age from a point source, and for a plane source is determined, and applied so that the sum of the slowing down densities due to an appropriate number of point sources will be equivalent to the result for a plane source.

The plane source assumptions are:

(1) an infinite plane emitting S neutrons per cm^2 per second with energy E_o.

(2) the source lies in the y, z plane passing through the origin, so that $q(x, y, z, \tau) = q(x, \tau)$.

Then $\nabla^2 q(x,\tau) = \frac{\partial q(x,\tau)}{\partial \tau}$ for $x \neq 0$.

and $q(x,o) = S\delta(x)$,

where $\delta(x)$ is again the Dirac delta function.

Assume separation of variables, so that

$$q(x,\tau) = X(x)T(\tau).$$

The age equation is then:

$$\frac{1}{X} \cdot \frac{d^2X}{dx^2} = \frac{dT}{d\tau} \cdot \frac{1}{T}.$$

Each side may be equated to a constant $-\alpha^2$, where α^2 must be a real positive quantity, since the slowing down density cannot increase with the increasing age of the neutrons.

Solutions are found to be

$$X = A \cos \alpha x + C \sin \alpha x,$$

$$T = Fe^{-\alpha^2 \tau}$$

and $$q = e^{-\alpha^2 \tau}(A \cos \alpha x + C \sin \alpha x).$$

These solutions are represented in an alternate form by use of the Fourier integral, by which

$$f(x) = \frac{1}{\pi} \int_0^\infty d\alpha \int_{-\infty}^\infty f(x') \cos\left[\alpha (x' - x)\right] dx'$$

where x' and α are independent of x and τ, so that they represent constants of integration.

Since, when $\tau = 0$, $q(x, \tau)$ must reduce to the Fourier integral of $S\delta(x)$, so q is represented by

$$q = \frac{1}{\pi} S\delta(x') e^{-\alpha^2 \tau} \cos\left[\alpha (x' - x)\right].$$

The linear age equation is then multiplied by $d\alpha dx'$ and integrated over all values of α and x' to obtain a complete solution. Thus,

$$q(x, \tau) = \int_0^\infty d\alpha \int_{-\infty}^\infty S\delta(x') e^{-\alpha^2 \tau} \cos\left[\alpha (x' - x)\right] dx'.$$

since $$q(x, 0) = S\delta(x) = \frac{1}{\pi} \int_0^\infty d\alpha \int_{-\infty}^\infty S \quad (x') \quad \cos\left[\alpha (x' - x)\right] dx'.$$

The integral with respect to α is

$$\int_0^\infty e^{-\alpha^2 \tau} \cos\left[\alpha (x' - x)\right] d\alpha = \sqrt{\frac{\pi}{4\tau}}\, e^{-(x' - x)^2/4\tau},$$

so $$q(x, \quad) = \frac{1}{\sqrt{4\pi\tau}} \int_{-\infty}^\infty S\delta(x') e^{-(x' - x)^2/4\tau} dx'.$$

Since $$\int_{-\infty}^\infty f(x') \delta(x') dx' = f(0),$$

$$q(x,\tau) = \frac{S}{\sqrt{4\pi\tau}}\, e^{-x^2/4\tau}$$

for a unit plane source.

It is seen from previous considerations that

$$q_{plane}\,(x,\tau) = \int_0^\infty q_{point}\,(r,\tau)\, 2\pi a\, da.$$

Since $x^2 + a^2 = r^2$ and $rdr = ada$, then

$$q_{pl}\,(x,\tau) = 2\pi \int_x^\infty q_{pt}\,(r,\tau) r dr.$$

$$\frac{dq_{pl}(x,\tau)}{dx} = -2\pi q_{pt}(x,\tau)x$$

or $$q_{pt}(x,\tau) = -\frac{1}{2\pi x}\,\frac{dq_{pl}(x,\tau)}{dx}.$$

But $$q_{pl}(x,\tau) = \frac{S}{4\pi\tau}\, e^{-x^2/4\tau}$$

and $$dq_{pl}(x,\tau) = -\frac{2xS}{4\tau\sqrt{4\pi\tau}}\, e^{-x^2/4\tau}$$

The last two equations give

$$q(r,\tau) = \frac{e^{-r^2/4\tau}}{(4\pi\tau)^{3/2}}$$

Or, to generalize for a unit point source at r_o with a field point at r,

$$q(r,\tau) = \frac{e^{-|r-r_o|^2/4\tau}}{(4\pi\tau)^{3/2}}.$$

By taking logarithms, it seen that for neutrons of a given energy, since τ is constant,

$$\ln q(r) = \text{constant}\left(-\frac{r^2}{4\tau}\right).$$

Thus, the plot of the logarithm of the saturated activity versus distance squared from the source will have a slope of $-\frac{1}{4\tau}$.

The deviation of the curve from the straight line near the source (52) is due to an appreciable number of neutrons present which have more than 1.46 ev energy. Thus, the experimental points for small r lie above the desired straight line.

The deviation found for large r (24) is because most neutrons in this region are thermalized, and the flux distribution varies as $e^{-k'r}$ rather than e^{-kr^2}.

Counting

Neutrons were detected by Indium foils and by BF_3 counter.

Equations for reactions involved in counting are:

$$In^{115} + {}_0n^1 \longrightarrow In^{116*}.$$

$$In^{116*} \xrightarrow{54.05m} In^{116} + {}_{-1}\beta^{\circ}. \qquad (68)$$

$$B^{10} + {}_0n^1 \longrightarrow B^{11*}. \qquad (31)$$

$$B^{11*} \longrightarrow Li^7 + \alpha.$$

It was difficult to obtain good counting statistics with foils since the polonium-beryllium source was rather weak.

Saturated activity was calculated by the equation (53)

$$A_s = Ct_3f$$

where C = counts/time observed

t_3 = counting time

$$f = \text{factor} = \left(\frac{1}{1-e^{-\lambda t_1}}\right)\left(\lambda e^{\lambda t_2}\right)\left(\frac{1}{1-e^{-\lambda t_3}}\right)$$

λ = decay constant

t_1 = activation time

t_2 = waiting time between removal of foil from pile until count is begun.

Resolving time error is given by (68).

$$R - R_o = \frac{R_o^2 \tau}{1-R_o\tau}$$

where R = true count rate, c/s.

R_o = observed count rate, c/s.

τ = resolving time, seconds.

The resolving time, τ may be found (68), by using two sources and the following relationship:

$$\tau = \frac{R_1 + R_2 - R_{12}}{2R_1R_2}$$

where R_1 = counting rate of source 1 (c/s)

R_2 = counting rate of source 2(c/s)

R_{12} = counting rate of both sources (c/s)

The true counting rate is the error plus the observed counting rate:

$$(R-R_o) + R_o = \frac{R_o^2\tau}{1-R_o\tau} + R_o$$

$$R = \frac{R_o(1-R_o\tau) + R_o^2\tau}{1-R_o\tau}$$

$$R = \frac{R_o}{1-R_o\tau}$$

The counting rate as determined by the Indium foils was low enough so that no dead time or resolving time corrections were needed.

FIG. 7 BLOCK DIAGRAMS OF COUNTING SYSTEMS

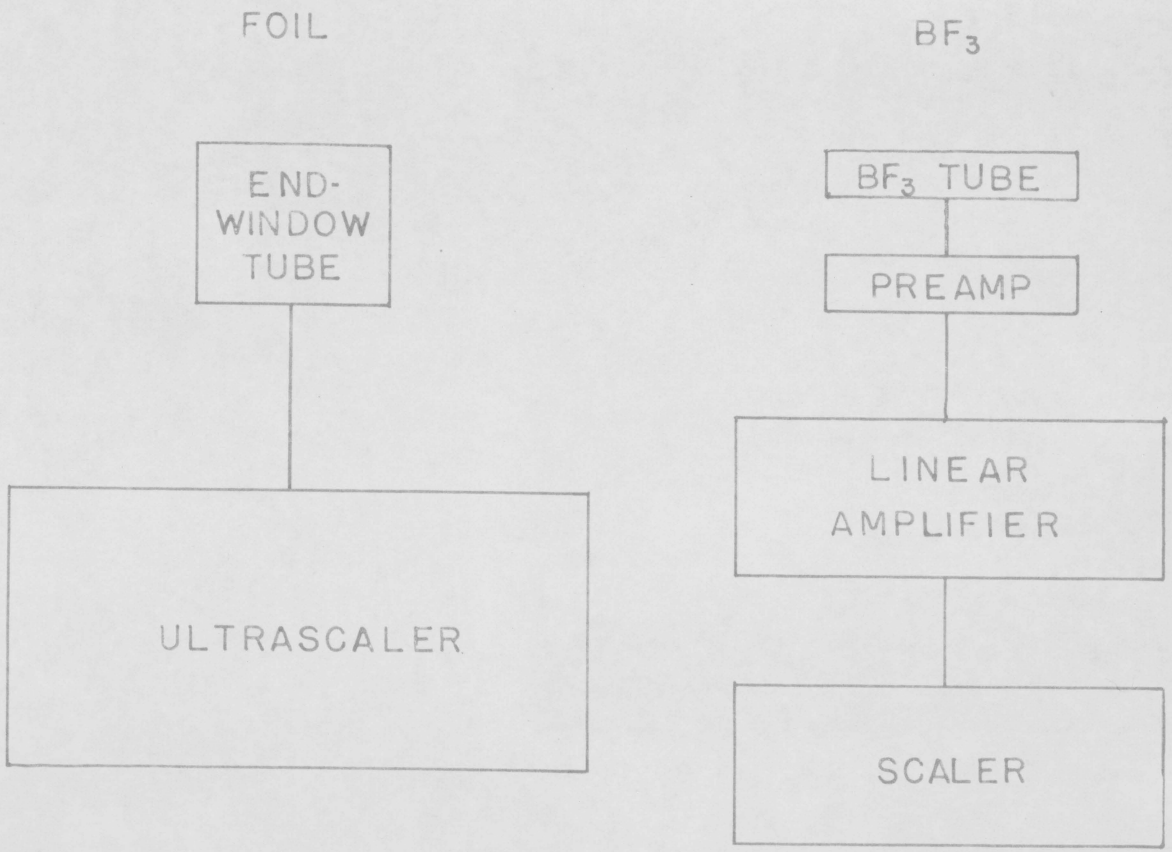

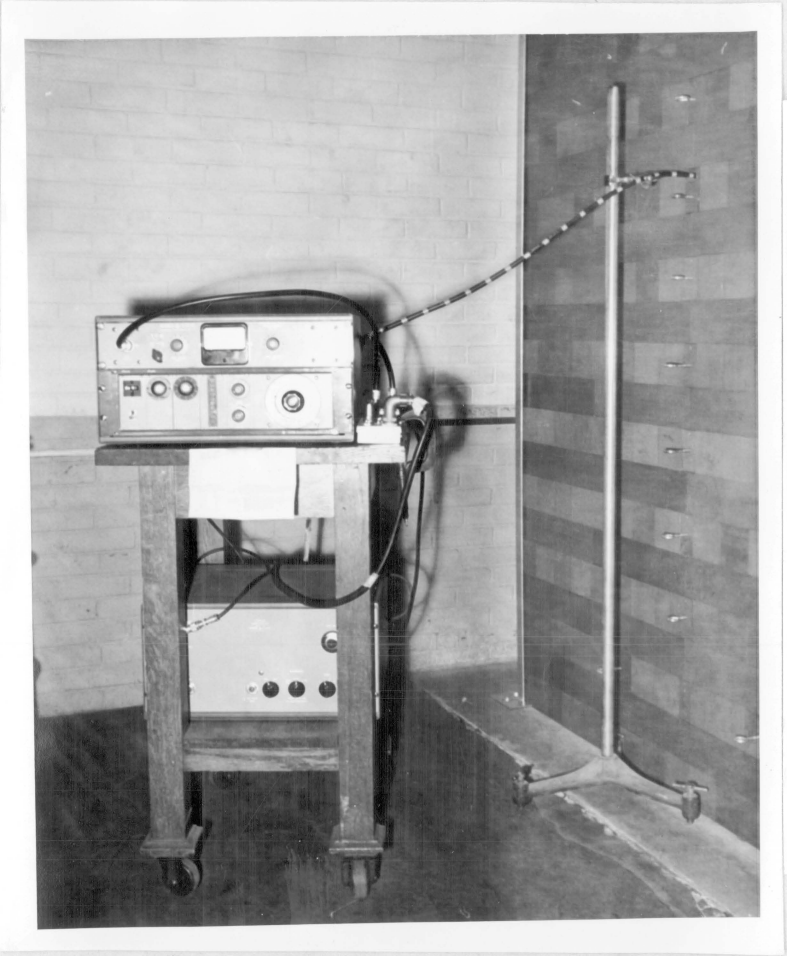

Fig. 7a BF_3 Detector Counting System

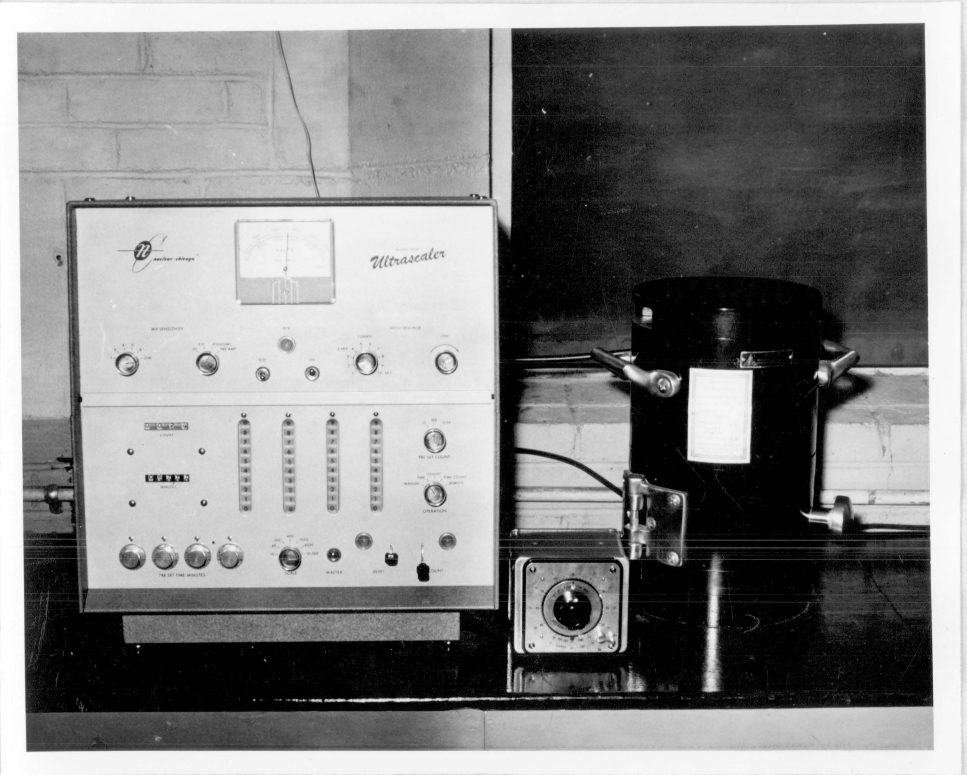

Fig. 7b Foil Counting System

VIII EXPERIMENTAL TECHNIQUES

Traverses

In order to determine the symmetry of the pile, both horizontal and vertical flux distributions were found.

A series of four horizontal BF_3 traverses were made from side "D" to side "B" in levels 13, 15, 17, and 19, using an RCL model 10503 detection tube. Four partial traverses were also made from the face of side "A".

In view of the indeterminate center of the sensitive volume of the BF_3 tube to obtain data which could be used for comparison at a later date, the base of the BF_3 tube, at its first point of contact with the outside of the cable connector from the counter was taken as a reference point. The cable was then calibrated in two inch sections for 56 positions. The face of the pile was used as the positioning point. Thus, the position referred to in the curves was determined as above.

Since the basic purpose of the BF_3 measurements was to prove the symmetry of the pile, no correction was made for resolving error. However, the manufacturer lists a rise time of 1-2 microseconds, and a fall time of 3-5 microseconds. This information should be used with the previous equations for computing the true counting rate, or other methods could be used to obtain a more accurate resolving time, such as using two sources, or oscilloscope techniques.

A rough diffusion length measurement was made from the horizontal

FIG. 8 HORIZONTAL TRAVERSE
SIDE "D" TO SIDE "B"

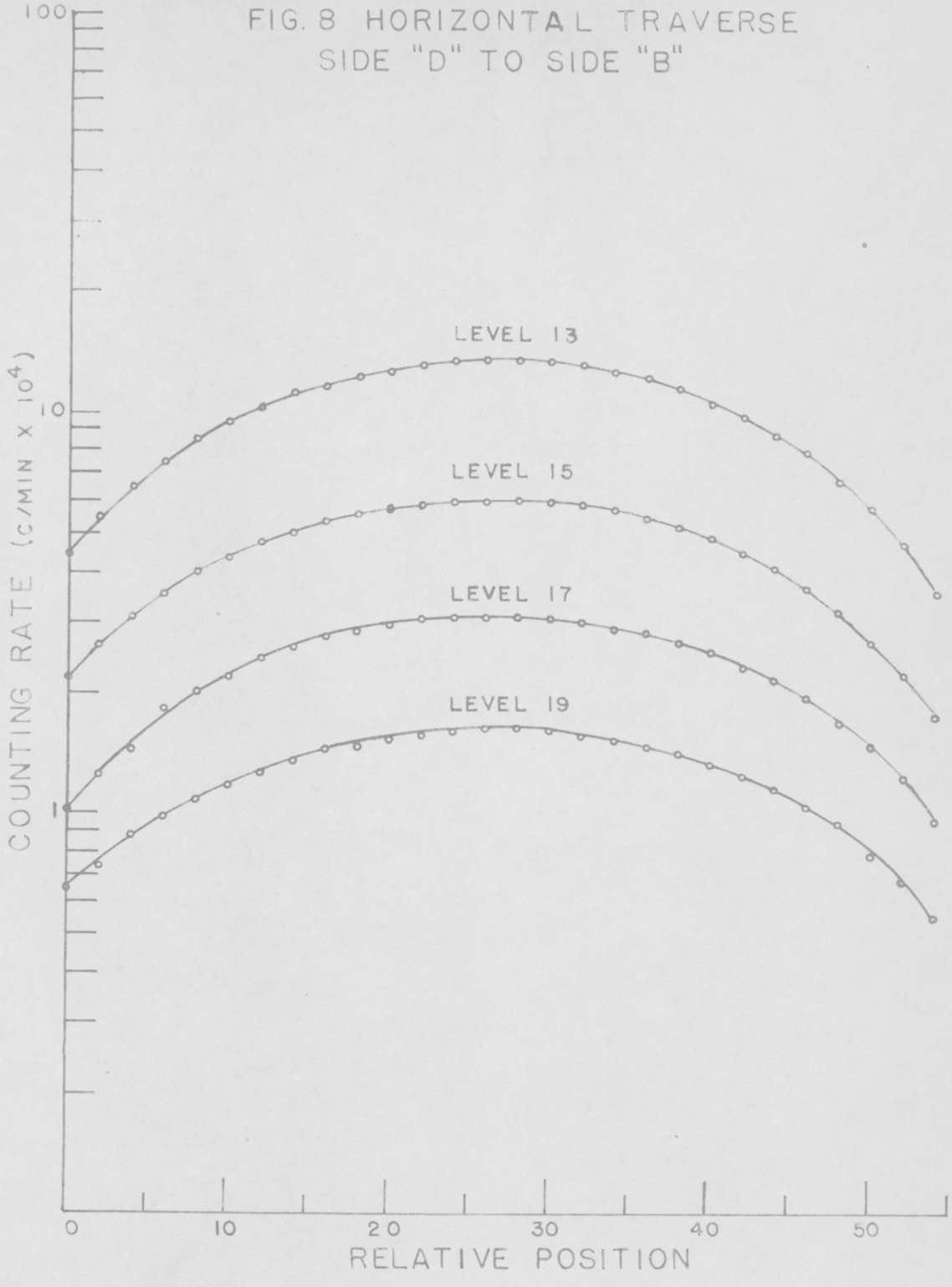

FIG. 9 PARTIAL TRAVERSE
SIDE "A"

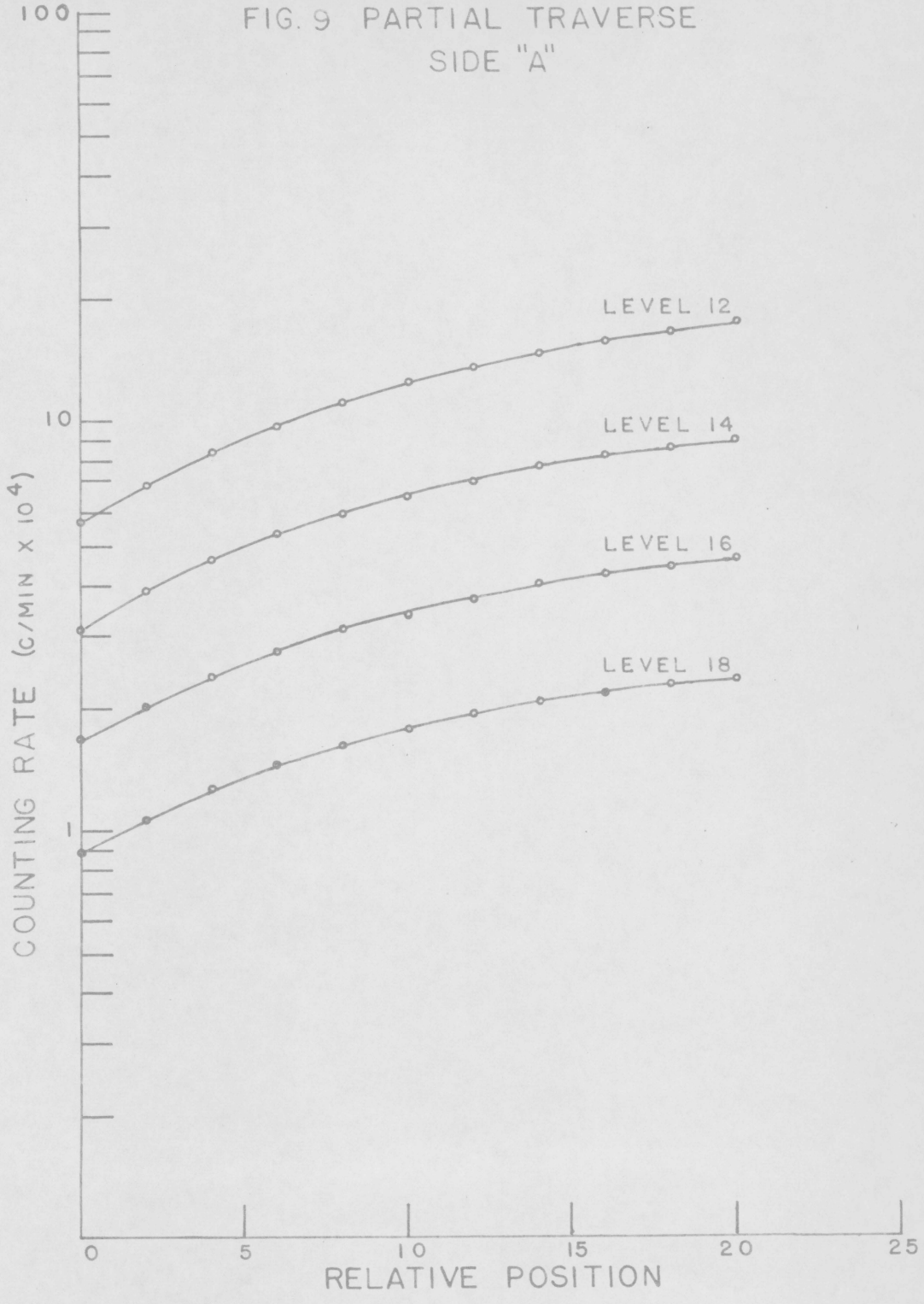

FIG. 10 VERTICAL TRAVERSE

POSITION TEN

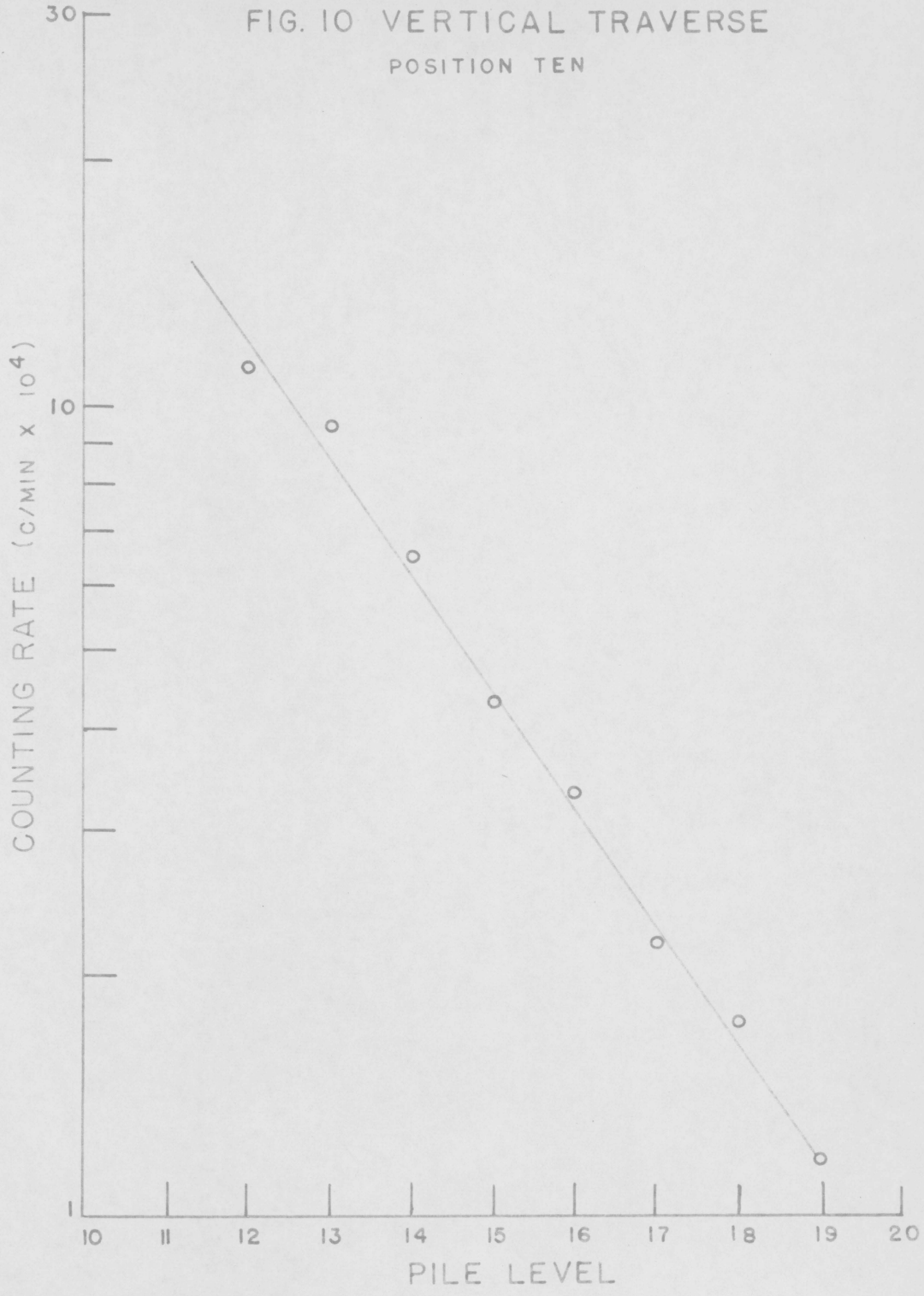

traverse data and gave a diffusion length of 53.3 cm, uncorrected for resolving time. Using a resolving time of five microseconds would decrease this value a maximum of approximately 1 1/2 per cent.

Data was taken from the horizontal traverses and used to construct a vertical flux distribution (or traverse).

Both horizontal and vertical traverses indicate the pile is symmetric.

Diffusion Length

Nineteen indium foils were irradiated to saturation in the pile and counted singly using an end-window counter and an Ultrascaler model 192A.

From a plot of ln saturated activity versus distance from the source, the slope of the curve was taken, and used to obtain the value (Appendix I) of 54.5 cm. $\pm$ 2cm for the diffusion length.

The plot of ln saturated activity versus distance from the source deviates from a straight line for points near the top of the pile because the term $e^{-2\gamma(c-z)}$ was neglected in the expression for ϕ. (28) If the measured fluxes are divided by $1 - e^{-2\gamma(c-z)}$, the logarithms of the corrected values will fall on a straight line for all values of z except the lowest.

Fermi Age

If indium foils are covered with cadmium covers, the effect of thermal neutrons is eliminated by absorption in cadmium, which undergoes an n,γ interaction. The foil so covered will give the relative values of the slowing down density at 1.46 ev. Indium actually has

FIG. II DIFFUSION LENGTH CURVE

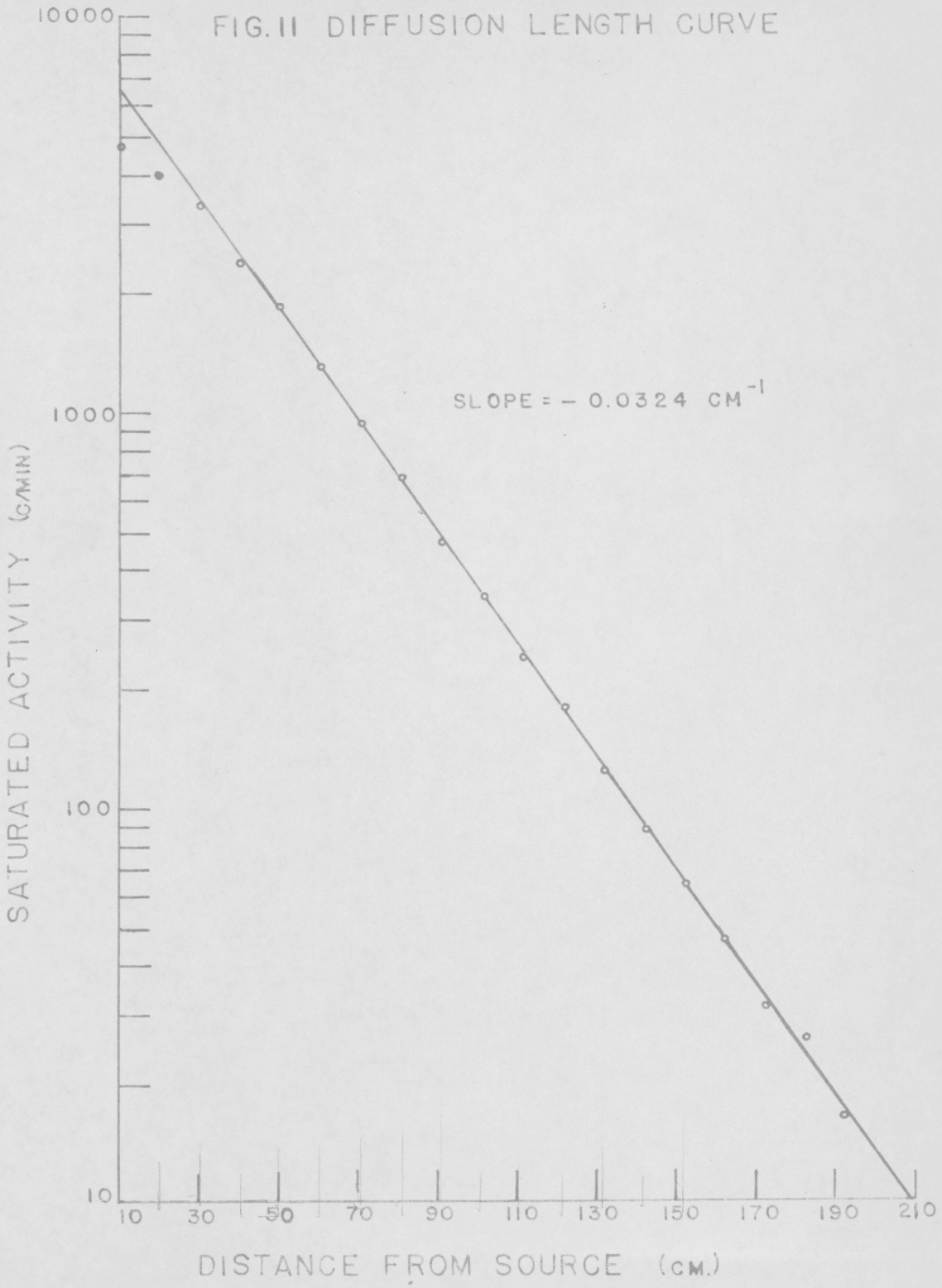

several minor resonances above this major one, but the effect of these is decreased with thin foils (40).

In this experiment, standard indium foils were placed between cadmium covers and irradiated in the pile for a length of time which was at least five or six times the half-life of indium (54.05 minutes). Thus, the foils were brought to saturation before counting. The foils were removed one at a time and counted with an end-window counter and an Ultrascaler Model 192A.

A curve was first plotted of all points taken, then fifteen foils were rerun to provide a check of the linear portion of the curve. A slight depression in activity at level eight was noted. Several runs were made at this point under the same conditions, and foils and blocks were also interchanged. No consistent trend was noted for any of these changes, and the average activity found by using the original components of level eight was plotted. Both curves were plotted using saturated activity as the ordinate and distance squared from the source plane as the abscissa (figure 12). It should be noted that a semilogarithmic plot of activity versus distance squared from the source plane (D^2) will have the same slope as a plot of activity versus straight-line distance squared from the source (R^2). Consider a right triangle of hypotenuse R, base S, and altitude D. Since $D^2 + S^2 = R^2$, as long as S^2 is constant, the above plot would only be displaced horizontally by changing the abscissa from D^2 to R^2, and the slope would remain the same. In the Sigma Pile, since the exact center of the pile occurs at the junction of two blocks, it was decided

to locate foil positions at a constant distance from the center, which was seven inches.

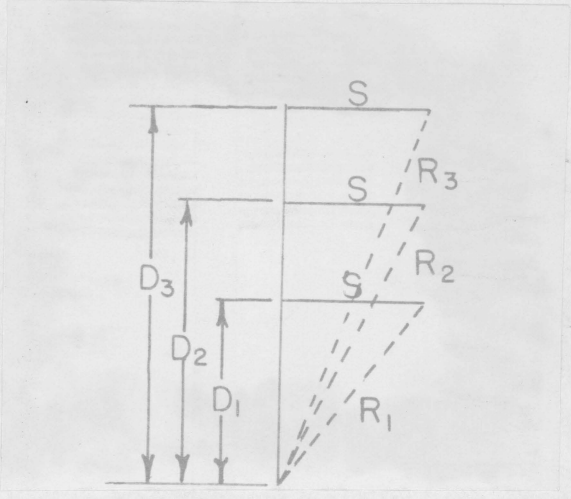

The agreement between both runs was good and led to a value of 330 cm^2 for the Fermi age at indium resonance, which is in agreement with earlier sources (29). A calculation (Appendix II) of τ from 1.46 ev to thermal energy (0.025 ev) gave 26.9 cm^2, thus giving a total age of 357 ± 5 cm^2, which is between earlier values of 350 cm^2 (29) (65) and later values of 364 cm^2 (51). Since the Fermi age depends on the properties of the graphite, the age is expected and has increased as the purity and density have been improved.

FIG. 12 FERMI AGE CURVE

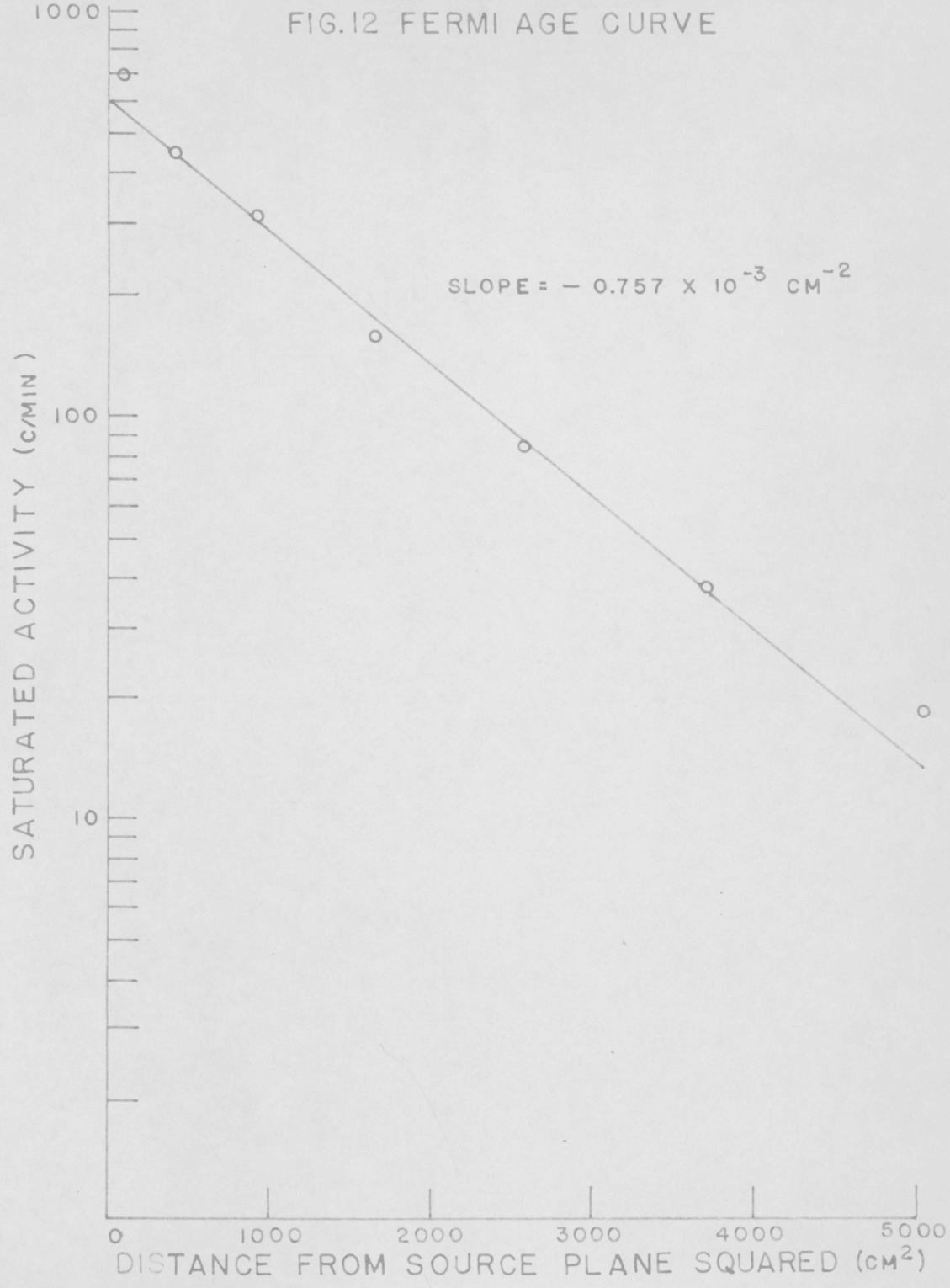

IX RESULTS AND SUMMARY

A Sigma Pile was constructed to serve as a laboratory facility at V.P.I.

Reproducible foil positions are possible with the positioning plates installed on the pile.

Withdrawal of the two outer blocks in each foil channel is facilitated by a coupling mechanism.

Five source positions permit operation with reduced harmonics.

The neutron distribution in the pile was proven to be symmetric by horizontal and vertical traverses.

By means of a diffusion length measurement, which gave an "L" of 54.5 ± 2 cm, and a Fermi Age measurement, which gave a "τ" of 357 ± 5 cm^2, the parameters of the pile were shown to be in good agreement with published data on graphite.

X ACKNOWLEDGMENTS

The author wishes to express his appreciation to the people who have assisted this investigation: To Dr. Andrew Robeson, for his guidance; to and the Physics Department shop force for their help in the machining operations; to , for typing this manuscript; and to his wife, , for her help and encouragement during this investigation and the preparation of this manuscript.

The author and the Physics Department are also indebted to the O'Sullivan Rubber Corp. for their generous donation of the plastic for the dust cover.

XI BIBLIOGRAPHY

1. Anderson, H. L., and E. Fermi, Production of Neutrons by Uranium, CPA-6. (As cited in reference 18.)

2. ANL-4174. Experimental Nuclear Physics Division Report for April, May, and June, 1948. (July 6, 1948)

3. Antonav, A. V., et al., "A Study of Neutron Diffusion in Beryllium, Graphite, and Water by the Impulse Method," Proceedings of the International Conference on the Peaceful Uses of Atomic Energy, Vol. 5, p/ 661, 1955.

4. Behrens, D. J., The Migration Length of Neutrons in a Reactor, AERE TR/877, 1952.

5. Behrens, D. J., "The Effect of Holes in a Reacting Material on the Passage of Neutrons, with Special Reference to the Critical Dimensions of a Reactor," Proc. Phys. Soc. (London), Vol. 62A, pp. 607-16, October 1949. (As cited in reference 60.)

6. Bethe, H. A., Nuclear Physics, Reviews of Modern Physics 9, pp. 71-244, 1937.

7. Block, E. Z., Reconciliation of Sigma Pile and 105 Pile Graphite Diffusion Lengths by Application of Neutron Streaming Corrections, H. W - 29147. (As cited in reference 59.)

8. Block, E. Z., and D. E. Davenport, Variation of Diffusion Length with Sigma-Pile Size, HW - 30422, January 4, 1954.

9. Branch, Garland M., Neutron Temperature Measurements in Graphite and in a Uranium-Graphite Reactor, MDDC-747, October 4, 1946.

10. Carlson, W. L., Neutron Age Measurements in Graphite with Gold Resonance Detection, ORNL - 784, November 7, 1950.

11. Chernick, J., and I. Kaplan, A Review of Graphite Testing Procedures and Their Applications to the BNL Reactor, BNL - 77, November 15, 1950.

12. Chernick, J., and R. S. Margulies, Sigma Pile Measurements on the Growing Brookhaven Reactor, BNL Log. No. 2604. (As cited in reference 11.)

13. Christy, R. F., The Slowing Down of Neutrons, Los Alamos Lecture Series, LA-24. (As cited in reference 10.)

14. Clayton E., Exponential Pile Measurements in the 7½" Lattice, HW - 28674. (As cited in reference 18.)

15. Currie, L. M., V. C. Hamister, and H. G. MacPherson, The Production and Properties of Graphite for Reactors, National Carbon Company, 1955.

16. Darrow, Karl K., Introduction to Diffusion-Theory and to Pile-Theory, AECD-3033 (CP-2475), October 6, 1944.

17. Davenport, D. E., G. L. Lynn, and D. C. Pound, Hanford Standard Pile, HW-21793, July 30, 1951.

18. Davenport, D. E., G. L. Lynn, and C. R. Richey, The Standardization (nv/q) of Gold and Indium Foils and the Absolute Neutron Flux Determination in the Hanford Standard Pile, HW-26207, August 27, 1954.

19. Duvall, G. E., Distribution of Thermal Neutrons in Exponential and Sigma Piles, HW-28268, June 3, 1953.

20. Fermi, E., J. Marshall, and L. Marshall, Slowing Down of Fission Neutrons in Graphite, CP-1084, (As cited in reference 11.)

21. Fite', Jose' Garcia, "Measurement of the Diffusion Length of Thermal Neutrons in Graphite," Nuclear Engineering, Part II, Chemical Engineering Progress Symposium Ser. No. 12, 11-15 (1954). (As abstracted in TID - 3070, Nuclear Science, A Bibliography of Selected Unclassified Literature.)

22. Friedman, F. L., Basic Theory for the Sigma Pile, M-4589, September 26, 1947.

23. Gast, P. F., Introduction to Pile Physics; Part One, HW-19474, November 15, 1950.

24. Glasstone, Samuel, and M. C. Edlund, The Elements of Nuclear Reactor Theory, D. Van Nostrand Co., New York, November 1952.

25. ibid, taken from pp. 90-127.

26. ibid, pp. 49-50, 115.

27. ibid, p. 123.

28. ibid, p. 126.

29. ibid, taken from pp. 174-183.

30. Hall, D., et at., Manual on Graphite Testing, CL-573. (As cited in reference 11.)

31. Halliday, David, Introductory Nuclear Physics, Second Edition, John Wiley & Sons, Inc., New York, 1955.

32. Havens, W. W. Jr., C. S. Wu, L. J. Rainwater, and C. L. Meaker, "Slow Neutron Velocity Spectrometer Studies II. Au, In, Ta, W, Pt, Zr," Phys. Rev. 71, pp. 165-173 (1947).

33. Havens, W. W. Jr., and J. Rainwater, "The Slow Neutron Cross Sections of Indium, Gold, Silver, Antimony, Lithium, and Mercury as Measured with a Neutron Beam Spectrometer," Phys. Rev. 70, pp. 154-173 (1946).

34. Hildebrand, F. B., Advanced Calculus for Engineers, Prentice-Hall, Inc., Englewood Cliffs, N. J., 1949.

35. Hochschild, R., Reactivity Test Facility for Uranium Slugs; Part I, Preliminary Report of a Non-Critical Assembly. (As abstracted in Nuclear Science Abstracts, Vol. 6, 3384, 1952.

36. Hochschild, R., Reactivity Test Facility, Part II. Proposal for a Sleeve Oscillator Test Reactor, AECD-3988, April, 28, 1953.

37. Hogg, C. H., and R. H. Lewis, MTR Flux Calibration Unit, IDO-16080, May 22, 1955.

38. Holmes, D. K., and R. V. Meghreblian, Notes on Reactor Analysis; Part II: Theory, CF-54-7-88, Issued August, 1955.

39. Honeck, Henry C., A Monte Carlo Calculation of the Fermi Age and Other Properties of the Slowing Down Distribution, CF 55-8-193, August, 1955.

40. Hughes, D. J., Pile Neutron Research, Addison-Wesley Publishing Co., Cambridge, Mass., 1955.

41. ibid, p. 214.

42. ibid, p. 213.

43. King, L. P. D., and R. E. Schreiber, Distribution and Power Measurements in the Water Boiler, AECD-3054, October 19, 1944.

44. Kerchner, R. M. and G. F. Corcorum, Alternating Current Circuits, Second Edition, John Wiley & Sons, Inc., New York, 1943.

45. Klema, Ritchie, and G. McCammon, Recalibration of the X-10 Standard Graphite Pile, ORNL-1398, AECD-3590, October 17, 1952.

46. Lee, M. T., Re-evaluation of Graphite Diffusion Lengths, HW-51175, June 5, 1957.

47. Legendre, P., et al., "The Production of Nuclear Graphite in France," Proceedings of the International Conference on the Peaceful Uses of Atomic Energy, Vol. 8, p. 343, 1955.

48. Maienschein, F., and W. B. Baker, Calibration of the NEPA Standard Pile, NEPA-1446. (As abstracted in Nuclear Science Abstracts, Vol. 8, 1690, 1954.)

49. Margulies, R. S., Initial Experiments on the Brookhaven Reactor; V: - Fast Source Correction for Sigma Piles, TID-5052, May 13,1949.

50. Montgomery, E. B., Diffusion Length Measurements in the DR and H Piles, HW-25261. (As cited in reference 60.)

51. Murray, Raymond L., Nuclear Reactor Physics, Prentice-Hall Publishing Co., Englewood Cliffs, New Jersey, 1957, p. 123.

52. Oak Ridge School of Reactor Technology, Reactor Physics Laboratory Manual, TID-5262, July, 1955.

53. Oleson, F. [illegible]., Neutron Monitoring with Indium Foils, BNL-351 (T62), July, 1955.

54. Pound, D. C., A. W. Thiele, and W. A. Cummins, Diffusion Length of Thermal Neutrons in Graphite - C Pile, HW-27553. (As cited in reference 59.)

55. Raievski, V., and J. Horowitz, "Determination of the Mean Transfer Free Path of Thermal Neutrons by Measurement of the Complex Diffusion Length," Proceedings of the International Conference on the Peaceful Uses of Atomic Energy, Vol. 5, p. 360, 1955.

56. Redman, C., Calibration of the New Argonne Standard Pile, AECD-3383, CP-3432, February 14, 1946.

57. Reddick, H. W. and F. N. Miller, Advanced Mathematics for Engineers, John Wiley & Sons, Inc., New York, p. 206.

58. Richey, C., Thermal Utilization and Lattice Diffusion Lengths in Graphite Uranium Lattices from Exponential Pile Measurements, HW-31305, AECD-3675, April 1, 1954

59. Richey, C. R., Diffusion Length Measurements in the 7½" Lattice Pile, HW-29748, October 26, 1953.

60. Richey, C. R., and E. Z. Block, Graphite Diffusion Length Measurements at Hanford, HW-45035, September 10, 1956.

61. Roberts, L. D., J. E. Hill, and G. McCammon, A Study of the Slowing Down Distribution of Sb^{124}-Be Photoneutrons in Graphite and the Use of Indium Foils, ORNL-201, February 24, 1950.

62. Sachs, D., B. Russell, A. Wattenberg, and R. Fields, "Yields of Neutrons From Photoneutron Sources," Phys. Rev. 73, 545-549, 1948.

63. Seren, L., Report on Argonne Standard Pile, CP-704. (As cited in reference 18.)

64. Soodak, H., and E. C. Campbell, Elementary Pile Theory, AECD-2201, John Wiley & Sons, Inc., New York, 1950.

65. Stephenson, Richard, Introduction to Nuclear Engineering, McGraw-Hill Book Co., Inc., New York, 1954, p. 141.

66. Thiele, A. W., and D. C. Pound, Diffusion Length of Thermal Neutrons in Graphite - K Piles, HW-35467. (As cited in reference 60.)

67. Tittle, C. W., "Slow Neutron Detection by Foils II," Nucleonics, Vol. 9, No. 1, pp. 60-67.

68. U. S. Department of Health, Education, and Welfare, Radiological Health Handbook, PB-121784, January 1957.

69. Volkoff, G., Notes on Cadmium Ratio Measurements, TPI-16. (As cited in reference 18.)

70. Weil, J. W., J. S. Levin, and R. S. Margulies, Diffusion Length Measurements on the Stacked Moderator, BNL Log No. C-3271. (As cited in reference 11.)

71. Weinberg, A. M., and L. C. Noderer, Theory of Neutron Chain Reactions: Vol. I, Diffusion and Slowing Down of Neutrons, CF 51-5-98, May 15, 1951.

72. Whitmore, B. G., and W. B. Baker, "The Energy Spectrum of Neutrons from a Po-Be Source," Phys. Rev. 78; 6, 799 1950.

The vita has been removed from the scanned document

XIII APPENDIX I

Table I. Diffusion Length Data

Foil No.	Level	Counts	Counting Time (min)	Transfer Time (min)	Back-ground	Corrected Counts	Foil Wt. Ratio	A_s
19	23	3,168	50.00	1	2564	604	1.0000	16.58
18	22	3,195	45.00	1	2307	888	1.0019	26.36
17	21	3,016	40.00	1	2051	965	1.0043	31.38
16	20	3,476	40.00	1	2051	1,425	1.0059	46.41
15	19	4,457	45.00	1	2307	2,150	1.0081	64.23
14	18	5,254	45.00	1	2307	2,947	1.0081	88.04
13	17	6,399	45.00	1	2307	4,092	1.0142	123.0
12	16	8,226	45.00	1	2307	5,919	1.0154	178.1
11	15	7,329	30.00	1	1538	5,791	1.0170	239.6
10	14	9,824	30.00	1	1538	8,286	1.0198	343.8
9	13	11,080	25.00	1	1282	9,798	1.0243	467.5
8	12	12,604	20.00	1	1025	11,579	1.0270	682.9
7	11	13,138	15.00	1	769	12,369	1.0138	930.9
6	10	12,183	10.00	1	513	11,670	1.0282	1295.
5	9	10,498	6.00	1	308	10,190	1.0294	1839.
4	8	11,336	5.00	1	256	11,080	1.0306	2388.
3	7	15,619	5.00	1	256	15,363	1.0323	3317.
2	6	11,263	3.00	1	154	11,109	1.0348	3957.
1	5	13,203	3.00	1	154	13,049	1.0394	4668.

XIII Appendix I (continued)

Calculation of Diffusion Length

$$\frac{1}{L^2} = \gamma_{\infty}^2 - \left(\frac{\pi}{\tilde{a}}\right)^2 - \left(\frac{\pi}{\tilde{b}}\right)^2$$

$$\tilde{a} = \tilde{b} = 66 \text{ in.} \times 2.54 \text{ cm/in.} + 2(.707)\lambda_{tr}$$

$$= 163.5 \text{ cm} + 2\ (.707)(2.60 \text{ cm})$$

$$= 167.2 \text{ cm.}$$

= Slope of ln saturated activity vs distance from source.

$$= -\left(\frac{\ln 6600 - \ln 10}{210\text{cm} - 10\text{cm}}\right)$$

$$= -\ 0.0324 \text{ cm}^{-1}$$

$$\frac{1}{L^2} = 10.5 \times 10^{-4} \text{ cm}^{-2} - 2\left(\frac{\pi}{167.2 \text{ cm}}\right)^2$$

$$= 3.42 \times 10^{-4} \text{ cm}^{-2}$$

$$L^2 = .292 \times 10^4 \text{ cm}^2$$

$$L = 54.0 \text{ cm}$$

Correcting for density (59),

$$L_{1.600} = \frac{1.617}{1.600} L_{1.617}$$

$$= \frac{1.617}{1.600} \cdot 54.0 \text{ cm}$$

$$L = 54.5 \text{ cm} \pm 2 \text{ cm}$$

XIII APPENDIX II

Table I. Fermi Age Data (first run)

Foil No.	Level	Counts	Counting Time (min)	Transfer Time (min)	Back-ground	Corrected Counts	Foil Wt. Ratio	As
15	19	4,376	80.00	1	4456	0	-	
14	18	4,336	80.00	1	4456	0	-	
13	17	4,453	80.00	1	4456	0	-	
12	16	4,541	80.00	1	4456	85	1.0000	1.726
11	15	4,757	80.00	1	4456	301	1.0016	6.120
10	14	4,724	80.00	1	4456	268	1.0044	5.464
9	13	4,623	80.00	1	4456	167	1.0088	3.420
8	12	5,004	80.00	1	4456	548	1.0114	11.25
7	11	5,489	80.00	1	4456	1,033	0.9984	20.94
6	10	6,357	80.00	1	4456	1,901	1.0126	39.08
5	9	8,451	80.00	1	4456	3,995	1.0138	82.22
4	8	10,090	66.00	1	3676	6,414	1.0150	144.9
3	7	11,561	40.00	1	2228	9,333	1.0167	307.2
2	6	13,978	34.00	1	1894	12,084	1.0191	452.7
1	5	10,018	15.00	1	836	9,182	1.0236	697.7

XIII APPENDIX II

Table II. Fermi Age Data

D^2 (cm^2)	A_s (First run)	A_s (Second run)	Re-runs	Average A_s
14,864	1.726			1.726
12,490	6.120			6.120
10,323	5.464			5.464
8,361.3	3.420			3.420
6,606.4	11.251			11.251
5,058.1	20.936	15.55		18.24
3,716.1	39.076	35.10	39.08, 35.10	37.09
2,580.6	82.218	82.77		82.49
1,651.6	144.888	143.70	167.06,150.06 152.2 ,162.5	153.9
929.03	307.233	314.48		310.9
412.90	452.747	440.65	440.2 ,440.65	443.6
103.25	697.743	696.56		697.15

XIII Appendix II (continued)

Calculation of Fermi Age

Calculation of Indium Resonance Age

$-\frac{1}{4\tau}$ = Slope of ln saturated activity vs distance squared.

$$= -\frac{\ln 600 - \ln 10}{5400\ cm^2} = -0.757 \times 10^{-3}\ cm^{-2}$$

$$= 330\ cm^2$$

Calculation of Age to Thermal from Indium Resonance (10)

$$\tau(E) = \int_{E}^{E_1} \frac{1}{3\xi\Sigma_s^2\left(1-\frac{2}{3A}\right)} \frac{dE}{E}$$

$$= \frac{1}{3\xi\Sigma_s^2\left(1-\frac{2}{3A}\right)} \ln \frac{E_1 .46}{E_t} \text{ if } \Sigma_s \text{ is independent of neutron energy.}$$

$$= \frac{1}{3(.158)(38.64 \times 10^{-2}\ cm^2)^2\left(1-\frac{2}{36}\right)} \ln \frac{1.46}{0.025}$$

$$\tau = 26.9\ cm^2$$

Calculation of Total Age

Total Age = Resonance Age plus Age to Thermal.

$$= 330\ cm^2 + 26.9\ cm^2 = 357 \pm 5\ cm^2$$